Tampere University

Jussi Isokuortti

NEW PORPHYRINS FOR EFFICIENT TTAUC IN VISCOUS SOLUTIONS

Faculty of Engineering and
Natural Sciences
Master's thesis
August 2019

ABSTRACT

Jussi Isokuortti: New Porphyrins for Efficient TTAUC in Viscous Solutions
Master's thesis
Tampere University
Science and Engineering
August 2019

Triplet-triplet annihilation upconversion (TTAUC) is an efficient process for photon upconversion: low energy light is absorbed and high energy light is emitted by the system. In this work, two different porphyrins, zinc and palladium tetraarylphthalimidoporphyrin (Zn and PdTAPIP), were utilized as sensitizers in TTAUC in two different viscous solvents, PEG200 and PEG300, providing viscosities of 54 and 520 cP, respectively. These high viscosity solvents were utilized as model systems for polymer matrices, such as micelles. High molar absorption coefficient and long triplet state lifetime of both porphyrin make them attractive for TTAUC. The performance of both porphyrin in both solvent was evaluated by determining quantum yield of upconversion and power density threshold. The properties of the porphyrins were additionally characterized by absorption, luminescence and quenching studies.

The thesis consists of two main parts. The first part is a literacy review of TTAUC divided into three chapters. The introduction takes a general look at photon upconversion and presents some applications and uses of TTAUC. Second and third chapters delve into the physical mechanisms and processes of TTAUC and the requirements for efficient TTAUC. Second part presents the experimental methods and measurement setups used to obtain the results that are shown and discussed in the last two chapters of the work.

This thesis establishes that both Zn and PdTAPIP are able to sensitize efficient TTAUC proven by high quantum yields of upconversion, low power density thresholds and large upconversion energy shifts even in viscous environments. PdTAPIP is capable of sensitizing TTAUC with slightly higher quantum yield and lower power densities than ZnTAPIP, the maximum quantum yield being 33 % in PEG200. However, after suppressing reverse triplet-triplet energy transfer, ZnTAPIP presents an intriguing case of efficient upconversion with 26 % quantum yield in PEG while exhibiting considerably endothermic energy transfer over a 3 k_BT energy gap resulting in large upconversion energy shift of 0,89 eV. With so high quantum yields and large upconversion energy shifts both porphyrin can be regarded as a state of the art sensitizer for TTAUC.

Keywords: photochemistry, upconversion, triplet-triplet annihilation, porphyrin

TIIVISTELMÄ

Jussi Isokuortti: Uusia porfyriineja tehokkaaseen ylöskonversioon viskooseissa liuoksissa
Diplomityö
Tampereen yliopisto
Teknis-luonnontieteellinen
Elokuu 2019

Tripletti-tripletti-annihilaatioon perustuva ylöskonversio (eng. triplet-triplet annihilation upconversion, TTAUC) on tehokas prosessi valon ylöskonversioon: matalaenergistä valoa absorboidaan ja korkeaenergistä valoa emittoidaan. Tässä työssä käytettiin kahta eri porfyriinia, sinkki- ja palladiumtetra-aryyliftaalimidoporfyriinia (Zn- ja PdTAPIP), herkistinaineina ylöskonversioon kahdessa eri viskoosissa liuottimessa, PEG200 ja PEG300, joiden viskositeetit olivat 54 ja 520 cP, vastaavasti. Näitä viskooseja liuottimia käytettiin mallintamaan polymeerimatriiseja, kuten misellejä. Molemmat porfyriinit ovat houkuttelevia herkistinaineita TTAUC:hen suurien molaaristen absorptiokertoimien ja pitkien triplettitilan elinaikojen ansiosta. Molemman porfyriinin suorituskykyä molemmassa liuottimessa arvioitiin määrittämällä ylöskonversion kvanttisaanto ja tehotiheyskynnys. Porfyriinien ominaisuuksia karakterisoitiin lisäksi absorptio-, luminesenssi- ja sammutustutkimuksilla.

Työ koostuu kahdesta osasta. Ensimmäinen osa on kirjallisuuskatsaus TTAUC:sta jaettuna kolmeen lukuun. Johdanto on yleinen katsaus ylöskonversioon sekä TTAUC:n käyttökohteisiin ja sovelluksiin. Toisessa ja kolmannessa luvussa paneudutaan TTAUC:n fysikaalisiin mekanismeihin ja prosesseihin sekä tehokkaan TTAUC:n edellytyksiin. Toisessa osassa esitellään työssä käytetyt kokeelliset menetelmät ja mittausjärjestelyt sekä tulokset ja niiden arviointi.

Diplomityö osoittaa molempien porfyriinien olevan toimivia herkistinaineita tehokasta TTAUC:ta varten, mitä todistaa suuret kvanttisaannot, matalat tehotiheyskynnykset ja suuret ylöskonversion energiasiirtymät. PdTAPIP on hieman suurempien kvanttisaantojen ja matalampien tehotiheyskynnysten myötä tehokkaampi herkistämään TTAUC:ta kuin ZnTAPIP suurimman kvanttisaannon ollessa 33 % PEG200:ssa. Kuitenkin ZnTAPIPin tulokset osoittavat, että ylöskonversio voi olla tehokasta, vaikka energiansiirto olisi huomattavan endotermistä 3 k_BT:n energiaraon yli. ZnTAPIPilla saavutettu ylöskonversioenergiasiirtymä oli 0,89 eV kvanttisaannon ollessa 26 % PEG200:ssa. Näin suurten kvanttisaantojen ja energiasiirtymien ansiosta molemmat porfyriinit ovat huipputason herkisitinaineita TTAUC:ta varten.

Avainsanat: valokemia, ylöskonversio, tripletti-tripletti-annihilaatio, porfyriini

PREFACE

This thesis was done during spring and summer of 2019 in the Supramolecular Chemistry of Bio- and Nanomaterials team in Tampere University. I want to thank our team for their help and support. I am especially thankful for the head of our team, professor Timo Laaksonen, for giving me the opportunity to prove myself as a chemist and privilege of studying chemistry while getting paid. To me it is quite special. I also thank my tireless mentor Dr. Nikita Durandin for instilling a passion for photochemistry in me and teaching me all I know about triplet-triplet annihilation in the lab and on the countless coffee breaks.

I thank Dr. Alexander Efimov for providing us pure compounds and for his skills in practical chemistry and storytelling. I thank Prof. Sergei Vinogradov at UPenn for collaboration and sending us his porphyrins. I also want to thank Prof. Nikolai Tkachenko, Dr. Elina Vuorimaa-Laukkanen and Dr. Terttu Hukka for numerous discussions about chemistry and physics.

I thank Markus, Timo and Tommi for making the university studies memorable and helping me pass physics and math with surprisingly good grades. Heikki and Oliver, I am always thankful for your lasting friendship. You have made Tampere feel like home to me. Cristina, thank you for your love and support, in thesis and in life. Äiti ja isä, you have made me the man I am today. I am truly blessed to have your help in everything and a second home in Hyvinkää.

Fiat lux.

Tampere, 12 August 2019

Jussi Isokuortti

CONTENTS

LIST OF SYMBOLS AND ABBREVIATIONS

2PA	Two-photon absorption
A	Annihilator
cP	Centipoise
DCM	Dichloromethane
FCWD	Franck-Condon weighted distribution of states
ISC	Intersystem crossing
OA	Oleic acid
PEAP	9-phenyl-10-(phenylethynyl)anthracene
PEG	Poly(ethylene glycol)
PUC	Photon upconversion
Q	Quintet state
QY	Quantum yield
RTET	Reverse triplet-triplet energy transfer
S	Sensitizer
SHG	Second-harmonic generation
SOC	Spin-orbit coupling
SV	Stern-Volmer (quenching relationship)
TAPIP	Tetraarylphthalimidoporphyrin
TTA	Triplet-triplet annihilation
TTAUC	Triplet-triplet annihilation upconversion
TET	Triplet-triplet energy transfer
UC	Upconversion
UES	Upconversion energy shift

[X]	Concentration of X, M
E	Energy, eV or k_BT
f	Spin-statistical factor
$\hat{H}$	Hamiltonian (operator)
I	Intensity or power density, mW/cm^2
k	Rate or rate constant
k_B	Boltzmann constant
K_{SV}	Stern-Volmer rate constant, M^{-1}
Z^{eff}	Effective nuclear charge
α	Absorption coefficient
γ_{TT}	Second-order decay rate of TTA
ΔE_T	Energy gap between sensitizer and annihilator triplet states, eV or k_BT
ΔH	Change in enthalpy
ϵ	Molar extinction coefficient, (M cm)$^{-1}$
Φ	Efficiency or quantum yield
Ψ	Wavefunction
τ	Lifetime, s
τ_0	Unquenched lifetime, s

1. INTRODUCTION

Photon upconversion (PUC) breaks the constraints of Stokes shift by absorbing low energy photons and emitting high energy ones, that can be utilized, for example, in harvesting solar energy or bioimaging and drug delivery. [1] This thesis seeks to make one particular PUC process, triplet-triplet annihilation (TTA) [2,3] as efficient as possible. Other notable PUC processes are two-photon absorption (2PA) [4,5] and second-harmonic generation (SHG) [6,7] that are based on the simultaneous absorption of multiple photons and upconversion by lanthanide ions [8,9] and cooperative energy pooling [10] that, as well as TTA, rely on metastable intermediate excited states capable of storing energy temporarily and transferring it to other states. What sets these latter processes apart from 2PA and SHG is the capability of working under lower power and under continuous-wave and non-coherent excitation sources, such as xenon lamp or sun. [1] As the earlier mentioned, this work focuses on triplet-triplet annihilation upconversion (TTAUC), which is the most efficient upconversion process in terms of quantum yield and power needed: TTAUC is capable of upconverting photons with multiple orders of magnitude higher quantum yields at lower power densities than, for example, lanthanide ion based upconversion systems. [1]

Triplet-triplet annihilation, also known as triplet fusion, was discovered in 1962 by Parker and Hatchard by observing blue-shifted and delayed fluorescence of naphthalene and anthracene after exciting phenanthrene or proflavin hydrochloride. [11] Interestingly, many of the other PUC processes mentioned above were also discovered in the 1960s thanks to many advances in science, such as the discovery of laser. Until the turn of the millennium, TTA remained a curiosity in photochemistry with sporadic reports mainly focused on the physical aspects of the process. With the development of more efficient triplet sensitizers, TTA has become progressively studied (see Figure 1) phenomenon with distinct applications. [1,12–18]

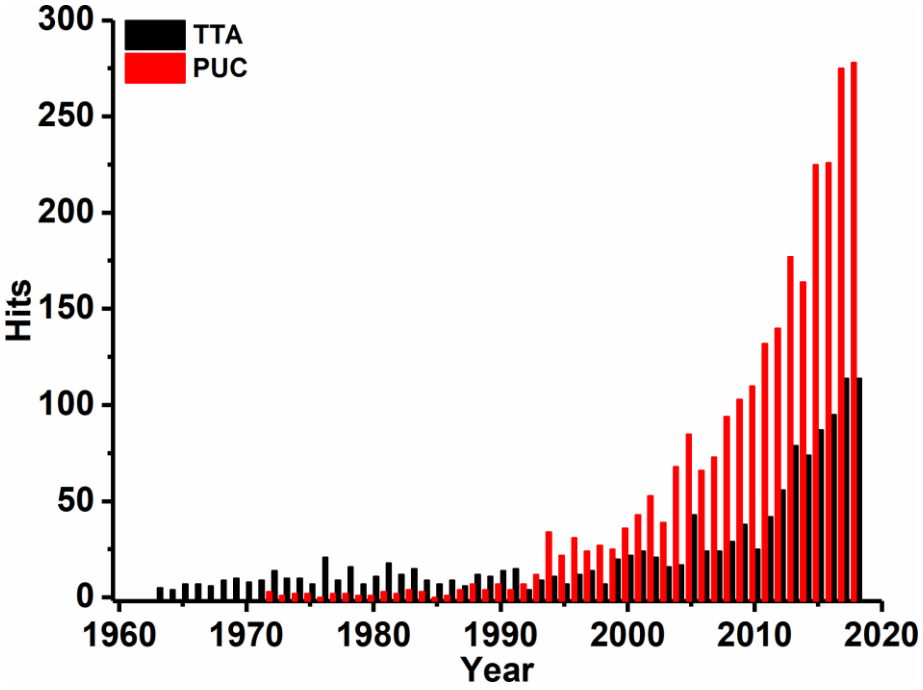

Figure 1. *Number of search results from article titles, abstracts and keywords on Scopus database with queries "triplet-triplet annihilation" (TTA) and "photon upconversion" (PUC). Results of the year 2019 are omitted from the graph.*

TTAUC has been proposed and investigated for solar cells [19–21] and photocatalysis [22] to utilize sub-band gap photons and thus enhance the efficiency of these devices. It has been estimated that upconversion-enhanced photovoltaic devices can have efficiencies up to 51 % [23,24]. TTAUC-driven photochemical reactions, such as cycloaddition [25] and photoisomerization for solar energy storage [26] and photoactuation [27], have also been demonstrated. Understanding and controlling TTA is also important for maximizing the efficiency of organic light-emitting diodes [28,29] and singlet fission materials [30].

Another prospective field of applications for TTAUC is in biomedicine, where longer wavelengths are needed to penetrate tissues and upconversion can provide higher energy photons for photoactivation or lower background noise in imaging. [17] These functions require embedding the active molecules into nanocapsules that carry the TTAUC system to the desired location of operation. Indeed, TTAUC has been successfully utilized in PMMA nanocapsules for *in vitro* imaging [31] and silica nanocapsules [32] and nanosized stabilized oil droplets [33] for *in vivo* imaging. Drug molecules can be released by photocleavage from a carrier or a carrier can be disrupted with light to release drug content in phototriggered drug delivery. [34] Both of these mechanisms require high energy photons that can be created *in situ* via TTAUC. Photocleavage driven by TTAUC has been demonstrated in liposomes [35,36] and polymer micelles [37,38].

Many of the applications of TTAUC mentioned here require encapsulation of the active molecules into a matrix. Depending on the application, the matrix is a polymer film, a viscous solvent like a liquid polymer or oil or a nanocapsule such as a micelle or a liposome. The viscosity of these materials plays a major role in the efficiency of TTAUC by restricting diffusion dependent processes but also protects the system from oxygen. It is thus prudent to study the TTAUC process and the performance of the active molecules in model viscous systems before advancing to “real” applications. In this work two liquid polymers, poly(ethylene glycol) 200 and 300 (PEG200 and PEG300), were used as viscous solvents for two porphyrins previously unused in TTA studies, palladium and zinc tetraarylphthalimidoporphyrin (Pd and ZnTAPIP), to study their performance in sensitizing TTA of 9-phenyl-10-(phenylethynyl)anthracene (PEAP) and achieve efficient TTAUC in these viscous solutions.

This work is compiled so that the physical mechanisms driving and affecting TTAUC are first reviewed before discussing what is required for efficient TTAUC and how maximum efficiency may be reached. After this rather theoretical examination the experimental methods are presented and finally the results are discussed with reflection to the relevance of this work. A photograph of one of the TTAUC systems studied is shown in Figure 2 as an appetizer for the reader.

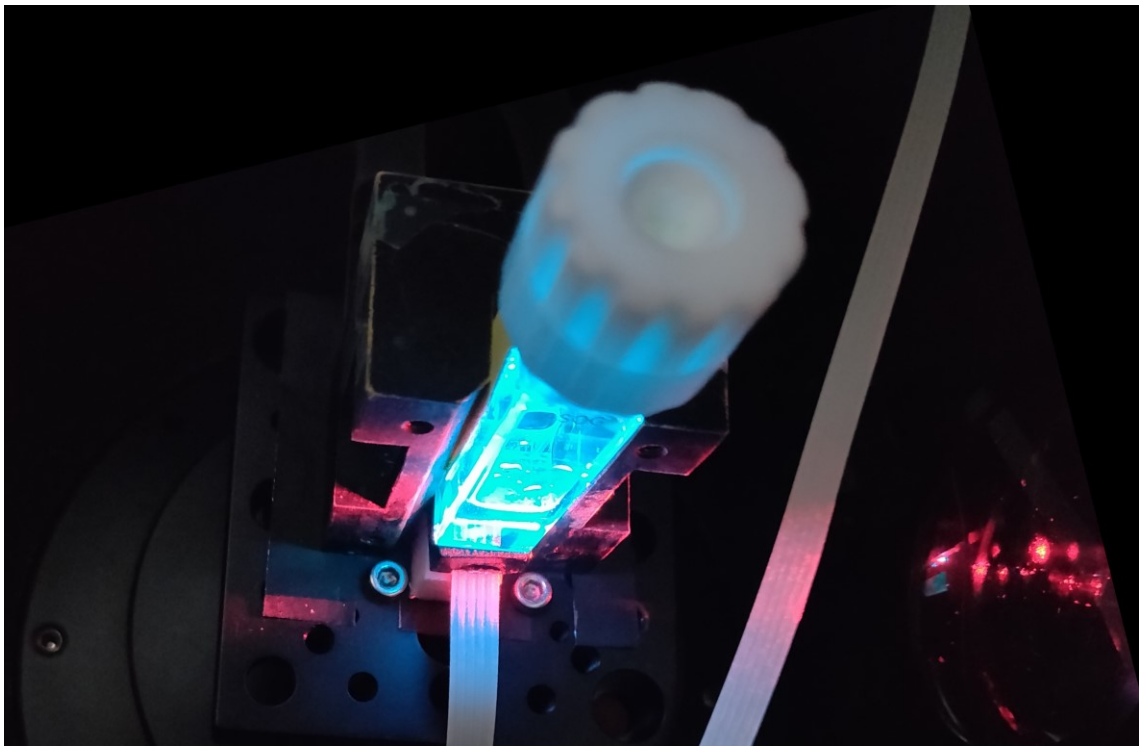

Figure 2. *PdTAPIP sensitized TTAUC in PEG200 upon red light (633 nm) excitation resulting in bright blue emission. Excitation is coming from the right.*

2. TRIPLET-TRIPLET ANNIHILATION UPCONVERSION

Studying any new phenomenon starts from definitions and fundamentals. This is at least the humble opinion of the author. Thus, appropriately, we will examine TTAUC step-by-step, discussing every distinct process of TTAUC starting from generation of a triplet state, transfer of this triplet state to another molecule and annihilation of triplet states resulting in delayed and upconverted fluorescence. These steps are shown in the scheme of TTAUC in Figure 3.

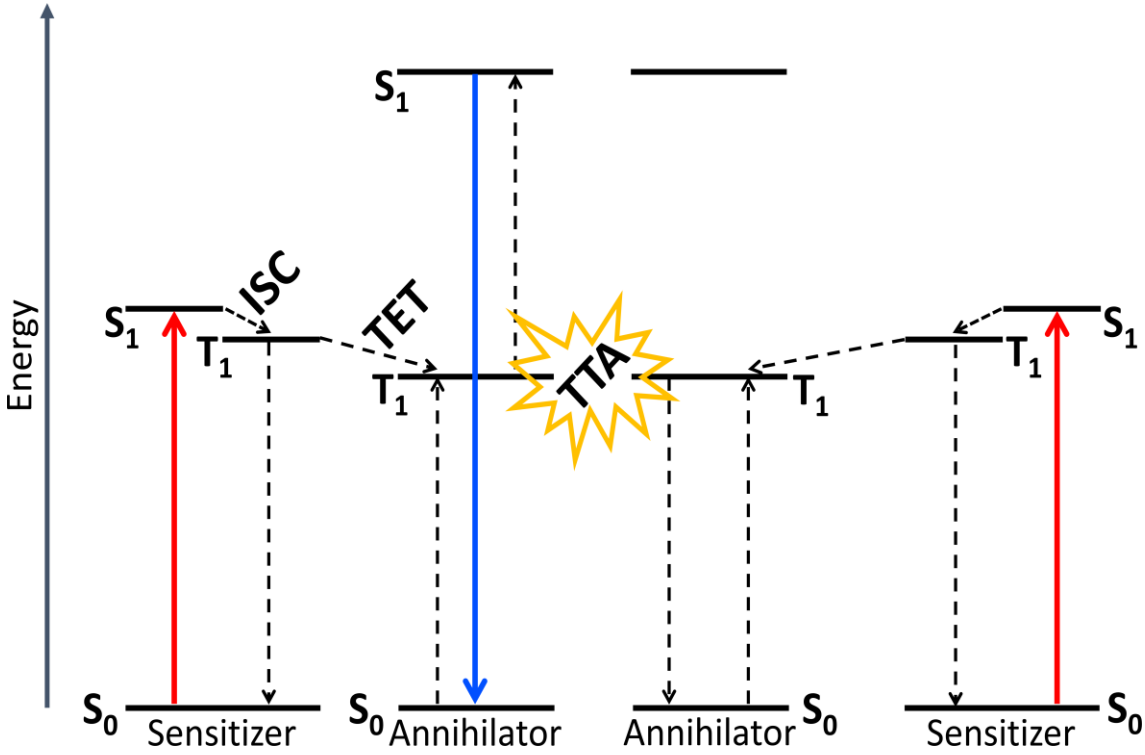

Figure 3. *A simplified scheme of TTAUC. First a sensitizer absorbs a lower energy photon (red arrow) and undergoes intersystem crossing (ISC) to yield an excited triplet state. This excited state (energy and multiplicity) is transferred to an annihilator molecule via triplet-triplet energy transfer (TET). Two triplet excited annihilator molecules then collide and upon collision occurs triplet-triplet annihilation (TTA) that creates one singlet excited annihilator that emits a higher energy photon (blue arrow) while the other annihilator reverts to its singlet ground state. All non-radiative transfers are marked with dashed arrows.*

2.1 Intersystem crossing

An excited state can decay via radiative, i.e. fluorescence and phosphorescence, or nonradiative processes, such as internal conversion, intersystem crossing and electron or energy transfer. [39] Since, generally, electronic transitions occur between states of equal spin multiplicity (1 and 3 for singlet and triplet states, respectively), a process called intersystem crossing is needed to yield a triplet state after exciting a molecule, such as a sensitizer in the case of TTA. Effective ISC is crucial for efficient TTAUC since the whole process depends on the triplet states generated by the sensitizer.

Spin-orbit coupling (SOC) mixes the singlet and triplet wave functions via a relativistic effect [40] on both angular momentum and spin thus allowing states of different multiplicities to couple. [39] In the context of photochemistry and photophysics, understanding SOC is essential, since it converts spin-forbidden transitions, intersystem crossing and phosphorescence, into allowed ones increasing their efficiency. [41]

Mathematically, the magnitude of SOC can be expressed as an integral over the singlet (Ψ_S) and triplet (Ψ_T) wave functions:

$$\left[\hat{H}_{SO}\right]_{ij} = \langle \Psi_{S_i} | \hat{H}_{SO} | \Psi_{T_j} \rangle, \quad (1)$$

where $\hat{H}_{SO}$ is the SOC operator or spin-orbit Hamiltonian. Presumably the most eminent SOC operator for one- and two-electron systems is the so called Breit-Pauli operator [42] which has two terms: The first describes the interaction between the orbiting electron and the nucleus and the second one describing the interactions of the electron with another one. In cases involving heavy elements, such as coordination complexes of noble metals, the two-electron contributions are included through the screening of the system's nuclear potential and thus the SOC operator is reduced into a quite simple form:

$$\hat{H}_{SO}^{eff} = \frac{1}{2m_e^2c^2} \sum_I \sum_i \frac{Z_{I,l}^{eff}}{\hat{r}_I^3} \hat{l}_{Ii} \hat{s}_i, \quad (2)$$

where m_e is the mass of the electron, c is the speed of light, I is an atom and i is an electron orbiting that atom, $Z_{I,l}^{eff}$ is the effective nuclear charge (i.e. the charge of the nucleus realized by the electron through screening), $\hat{r}$ is the distance of the electron from the atom, $\hat{l}_{Ii}$ is the angular momentum of the electron and $\hat{s}_i$ is the spin operator of the electron i. [39] It is worth mentioning, that in computation the values of $Z_{I,l}^{eff}$ are fitted to experimental atomic data provided by, for example, fine-structure splitting. [43]

As we can see in Eq. 2, the SOC operator depends on the effective charge of the nucleus. Indeed, the effect of larger atomic number on probability of spin-forbidden

transitions was first reported by McClure in 1949 [44]. This effect is also known as the heavy-atom effect and it is the most straightforward explanation for increased rates of singlet-triplet transitions. SOC matrix elements are approximately proportional to $\left(Z^{eff}\right)^4$ and therefore one might conclude that spin-orbit interactions, and as a result intersystem crossing, increase down the periodic table. However, this approximation cannot describe the extent of spin-forbidden transitions in some cases, for example when the energies of the singlet and triplet states are close. [39]

The discussion above was limited to specific nuclear coordinates. However, in many cases, such as polyatomic molecules with energetically close-lying electronic states and many nuclear degrees of freedom, the electronic and nuclear motion cannot be separated (as per Born-Oppenheimer approximation [45]). This means that the electronic and nuclear motion are coupled and this vibronic coupling can manifest itself as, for example, conical intersections where nonadiabatic transitions between electronic states can occur in ultrafast (femtosecond) timescales. [46]

Additionally, electronic states are mixed by both SOC and vibronic coupling resulting in total coupling called spin-vibronic coupling [39] that can be described with three distinct mechanisms [47]: 1) vibrational coupling depending on the nuclear degree of freedom, 2) spin-vibronic coupling with vibronic coupling in the triplet manifold and 3) spin vibronic coupling with vibronic coupling in the singlet manifold. Thus, the total mixing of the triplet and singlet states is the sum of spin-vibronic coupling depending on nuclear coordinates of the system and SOC (as described above) depending on the electronic character of the states.

Qualitatively, ISC may be characterized with a few different approaches. Fermi's golden rule is generally used to describe rates of population transfer between states close in energy. [48] With perturbation theory, this approximation can be written as

$$k = \frac{2\pi}{\hbar}\sum_f \left|\left\langle \Psi_f \middle| \hat{H}_{if} \middle| \Psi_i \right\rangle\right|^2 \delta(E_i - E_f), \quad (3)$$

where Ψ_f and Ψ_i are the vibronic and electronic wave functions of the final and initial states, $\hat{H}_{if}$ is the Hamiltonian describing the coupling between these states (in case of ISC, this Hamiltonian is $\hat{H}_{SO}$ as in Eq. 1). The δ function is used to ensure the conservation of energy in a nonradiative transition. In case of pure SOC, the wave functions are separable into electronic and vibrational parts:

$$k = \frac{2\pi}{\hbar}\sum_f \left|\left\langle \Psi_f \middle| \hat{H}_{if} \middle| \Psi_i \right\rangle\right|^2 \sum_k \left|\left\langle \nu_{fk} \middle| \nu_{ia} \right\rangle\right|^2 \delta(E_i - E_f). \quad (4)$$

This highlights the importance of electronic and vibrational contributions for the ISC rate.

One attempt to describe the remarkable ISC efficiency in nitrogen heterocyclics in absence of heavy atoms was made by El-Sayed [49] in 1963. This work is nowadays known prevalently as *El-Sayed's rules* and they predict that ISC in case of ${}^3(n\pi^*) \leftarrow {}^1(\pi\pi^*)$ is faster than in ${}^3(\pi\pi^*) \leftarrow {}^1(\pi\pi^*)$, i.e. for effective ISC, the change of spin state requires change in angular momentum thus conserving total angular momentum ($\hat{J} = \hat{L} + \hat{S}$). El-Sayed's rules are suitable for estimating ISC rates in many cases, such as metal-to-ligand charge transfer in metal-organic complexes, yet it should be mentioned that they are based on pure electronic states and thus vibronic coupling can break down these rules and lead to so called El-Sayed forbidden ISC. [39] Still in some of these cases El-Sayed rules can be used, at least partially, to explain enhanced ISC efficiency. One example of this is free-base porphyrin, where out-of-plane vibrations mix some σ character into the otherwise purely $\pi\pi$ orbitals, thus increasing ISC efficiency. [50] Although the porphyrins used as sensitizers for TTAUC typically are coordinated with heavy atoms, these vibrational effects still have an effect in their ISC which further attests the importance of understanding vibrational contributions to ISC.

Vibronic coupling can be estimated with overlap of initial and final vibrational density of states or so called Franck-Condon weighted density of states (FCWD) which can be written as: [51]

$$FCWD = \frac{1}{\sqrt{4\pi\lambda k_b T}} \exp\left[-\frac{(\Delta E+\lambda)^2}{4\pi\lambda k_b T}\right], \quad (5)$$

where λ, in case of ISC, is the energy difference between the singlet equilibrium geometry and the triplet at the singlet geometry (a vertical transition between the states) and ΔE is the energy gap between the minima of singlet and triplet state and the driving force of the reaction. Eq. 5 outlines two instances of nonradiative transitions introduced by Jortner and Engleman [52], namely the weak coupling limit and the strong coupling case. In the weak coupling limit, the change in geometry (reaction coordinates) associated with the transition is small (and thus λ is small) so the rate (probability) of the transition depends exponentially on ΔE, meaning that the rate is larger when ΔE is smaller. This relation between the rate of transition and the energy gap is called reasonably the *energy gap law*. When the potentials of the states are not nested i.e. the transition involves a substantial change in reaction coordinates and an intersection between the two potentials is to be expected, the strong coupling case is characterized by the rate of transition having a Gaussian dependency on $\Delta E + \lambda$.

After ISC, there are generally two pathways for the sensitizer to revert to its singlet ground state. The sensitizer can either decay through phosphorescence or, in presence of another molecule, donate the energy and multiplicity via triplet-triplet energy transfer.

2.2 Triplet-triplet energy transfer

When a triplet state is yielded after photoexcitation and subsequent ISC, the energy and spin state of the excited sensitizer molecule (S) is transferred to an annihilator molecule (A) via triplet-triplet energy transfer (TET) first quantitatively described by Terenin and Ermolaev [53] in 1952. With a reaction equation, it can be expressed as

$$^3S + {}^1A \rightleftharpoons {}^1S + {}^3A. \quad (6)$$

An equilibrium arrow is used since in some cases reverse triplet-triplet energy transfer (RTET) may be substantial. The energy balance of this transfer is

$$\Delta E_T = E_T^A - E_T^S, \quad (7)$$

where $E_T^S = E(\,^3S \rightarrow {}^1S)$ and $E_T^A = E(\,^1A \rightarrow {}^3A)$. It should be noted, that ^3S and ^1A denote the S and A molecules at their respective equilibrium geometries (pertaining to vertical transitions in a potential energy scheme). [54]

Generally, TET is thought to happen in the form of Dexter two-electron exchange [55] (see Figure 4) where the energy is transferred within an encounter complex $[S \cdots A]$. For this encounter complex formation and subsequent energy transfer, the molecules need to be at a collision distance (< 1 nm) from each other. [54] Quantum mechanically, the energy transfer rate can be expressed as [56–58]

$$k_{ET} = \frac{2\pi}{\hbar} U^2 J = \frac{2\pi}{\hbar} U^2 \int F_S(E) f_A(E)\, dE\,, \quad (8)$$

where U is an electron exchange (coupling) integral between the S and A in their electronic configurations in the initial (S at triplet and A at singlet) and final (S at singlet and A at triplet) states and J is a vibrational term that can be evaluated using the overlap (akin to Förster resonance energy transfer [59]) of normalized phosphorescence ($F_S(E)$) and $^1A \rightarrow {}^3A$ absorption* ($f_A(E)$) spectra of S and A, respectively.

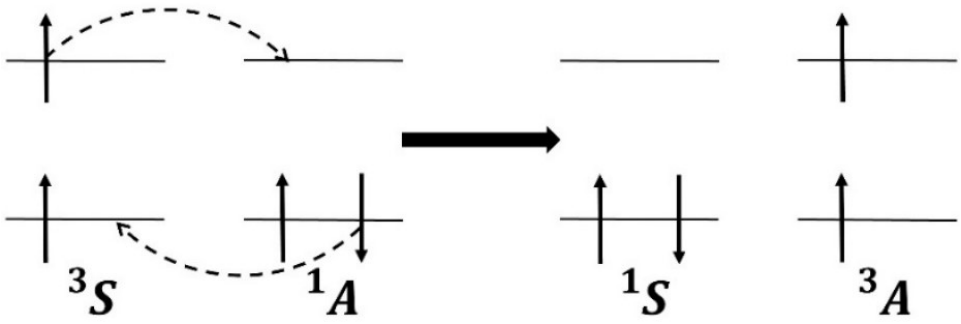

Figure 4. *Scheme of TET via Dexter two-electron exchange.*

The function $f_A(E)$ is somewhat problematic in Eq. 8: Experimentally it is difficult to determine due to the transition being spin-forbidden and thus very weak. Theoretically it is challenging to define to what extent absorption is analogous to electron exchange since the mechanisms are different. [58]

Furthermore, the electron exchange integral U can be defined as [58]

$$U^2 = K^2 \exp\left(-\frac{2R}{L}\right), \quad (9)$$

where K is a constant with a dimension of energy, R is the distance between S and A and L is a constant called effective average Bohr radius. This exponential dependence to distance stems from the generally exponential decline of molecular wavefunctions.

On a more macroscopic level, TET can be studied with the means of thermodynamics and kinetics. In an exothermic case, where the annihilator triplet energy is substantially lower than the sensitizer's ($\Delta E_T \leq -4$ k_BT), the rate of TET is diffusion-controlled (see Figure 5). This holds particularly well for TET in viscous solvents, since molecular encounters last longer while in lower viscosity solvents, such as toluene, rate of TET is substantially smaller than the rate of diffusion. [60,61][a] Thus, the TET rate constant for a given S and A pair can be simplified to [61]

$$k_{TET} \approx k_{diff} \propto \frac{1}{\eta}, \quad (10)$$

where k_{diff} is the rate constant of diffusion, which according to the Einstein relation [62] is inversely proportional to dynamic viscosity η.

As the energy gap between the S and A triplet states becomes smaller, the transfer probability decreases and k_{TET} becomes smaller than k_{diff} (see Figure 5). [63,64] In this case, as the enthalpic driving force of the reaction diminishes, the rate of TET can be separated from the rate of diffusion and expressed with an Arrhenius [65] type equation [66]:

$$k_{TET} = k_{diff} \frac{1}{1+\exp\left(\frac{\Delta E_T}{k_B T}\right)}. \quad (11)$$

Even in an endothermic case (ΔE_T > 0), where the annihilator triplet energy is up to 5 k_BT (at room temperature) or 130 meV higher than sensitizer's, TET still occurs, but at considerably smaller rate (see Figure 5). [54] In endothermic TET, the vibrational contributions of the molecules become more pronounced. [54,66]

[a] As the diffusion is slower in higher viscosity, the molecular encounters last longer. While molecular encounters are more probable in low viscosity, in viscous solvent the probability of energy transfer occurring *during* a molecular encounter is higher than in lower viscosity solvents. Thus, in higher viscosity the rate of energy transfer approaches the rate of diffusion.

In this endothermic region reverse triplet-triplet energy transfer becomes significant. In RTET energy is transferred back to S from A, which is naturally detrimental to TTAUC since overall A triplet population decreases. RTET occurs via the same mechanisms as TET and thus abides by the same Arrhenius type equations. The rate of RTET at a thermal equilibrium between S and A is [66]

$$k_{RTET} = k_{diff} \frac{\exp\left(\frac{\Delta E_T}{k_B T}\right)}{1+\exp\left(\frac{\Delta E_T}{k_B T}\right)} = k_{TET} \exp\left(\frac{\Delta E_T}{k_B T}\right). \quad (12)$$

In a more thorough thermodynamic examination of TET, it should be noted that change in enthalpy (ΔH) is not the only driving force in a thermodynamic process. Cheng et al. [67] have shown, that RTET can be suppressed with higher A ground state and S triplet state concentration in the system since the change in entropy increases as they increase:

$$\Delta S = k_B \ln\left(\frac{[\,^1A][\,^3S]}{[\,^1S][\,^3A]}\right). \quad (13)$$

Eq. 13 can quite simply be explained with probabilities: high A ground state concentration increases probability of TET, while higher S triplet state concentration prevents RTET. This is explanation is expanded in Figure 6. The increased change in entropy then can make a process exergonic even if ΔH is positive ($\Delta G = \Delta H - T\Delta S$). Eq. 13 presents ways of suppressing RTET, which are discussed further in chapter 3.2.

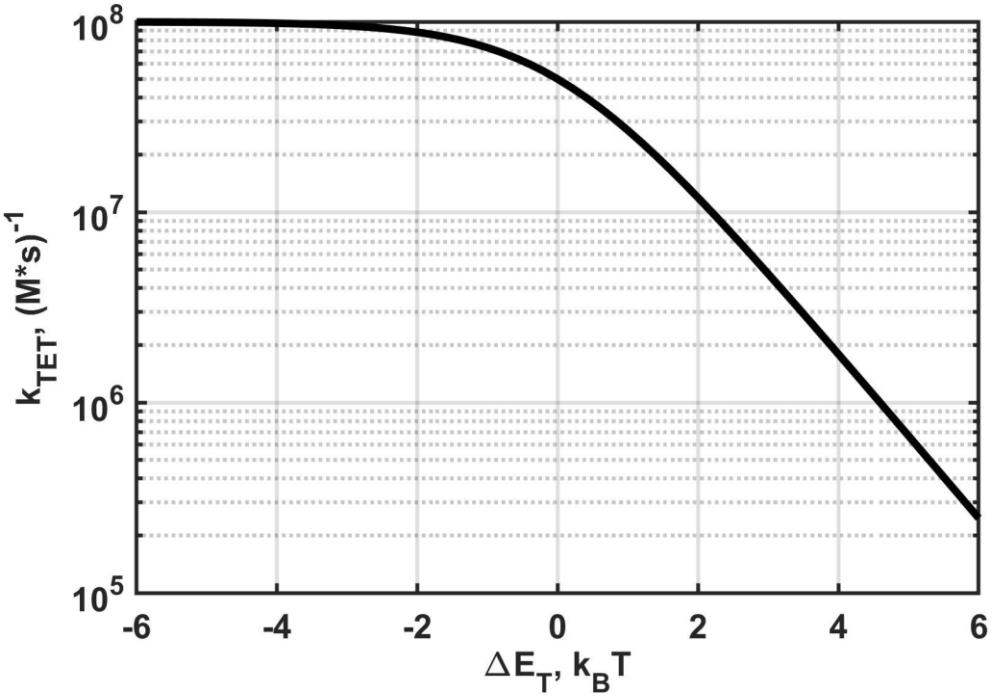

Figure 5. *Triplet-triplet energy transfer rate k_{TET} in solvent with $k_{diff} = 10^8\ (M\ s)^{-1}$ at different triplet energy gap (ΔE_T) values according to Eq. 11. For reverse triplet-triplet energy transfer the plot would be the same if the horizontal axis was opposite. The plots would intercept at $\Delta E_T = 0$ and thus $k_{TET} = k_{RTET} = \frac{1}{2} k_{diff}$.*

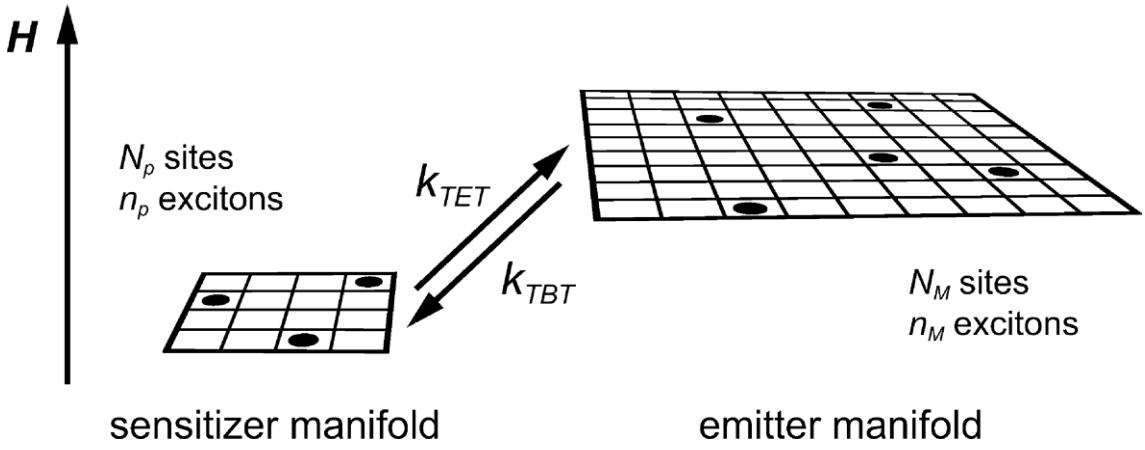

Figure 6. *Eq. 13 can be explained with empty and filled sites in sensitizer and annihilator (emitter in the figure) manifolds. By increasing the annihilator ground state concentration, the probability of TET is increased as the annihilator manifold grows. RTET (TBT in figure) is conversely inhibited by decreasing the number of "empty" sites in sensitizer manifold. This can be achieved by decreasing sensitizer ground state concentration or filling the sites with triplet excited states (excitons). With longer living triplet state, the probability of the sensitizer sites being filled at any given time is increased. Reprinted with permission from* [67]*. Copyright (2011) American Chemical Society.*

Experimentally, TET can be studied by measuring phosphorescence intensity or lifetimes (τ) of sensitizer with different annihilator concentrations. The ratio of unquenched phosphorescence lifetime (τ_0) to quenched lifetime depends on the Stern-Volmer relationship [68]:

$$\frac{\tau_0}{\tau} = 1 + K_{SV}[A], \tag{14}$$

where $[A]$ is the total concentration of annihilator and, in case of TET, $K_{SV} = k_{TET}\tau_0$. The efficiency of TET (Φ_{TET}) is defined as

$$\Phi_{TET} = 1 - \frac{\tau}{\tau_0}. \tag{15}$$

Using Eq. 14 ($\frac{\tau}{\tau_0} = \frac{1}{1+k_{TET}\tau_0[A]}$), we can rewrite Eq. 15:

$$\Phi_{TET} = \frac{k_{TET}[A]}{\frac{1}{\tau_0}+k_{TET}[A]}. \tag{16}$$

The effect of annihilator concentration on triplet-triplet energy transfer efficiency at two different ΔE_T and τ_0 is shown in Figure 7.

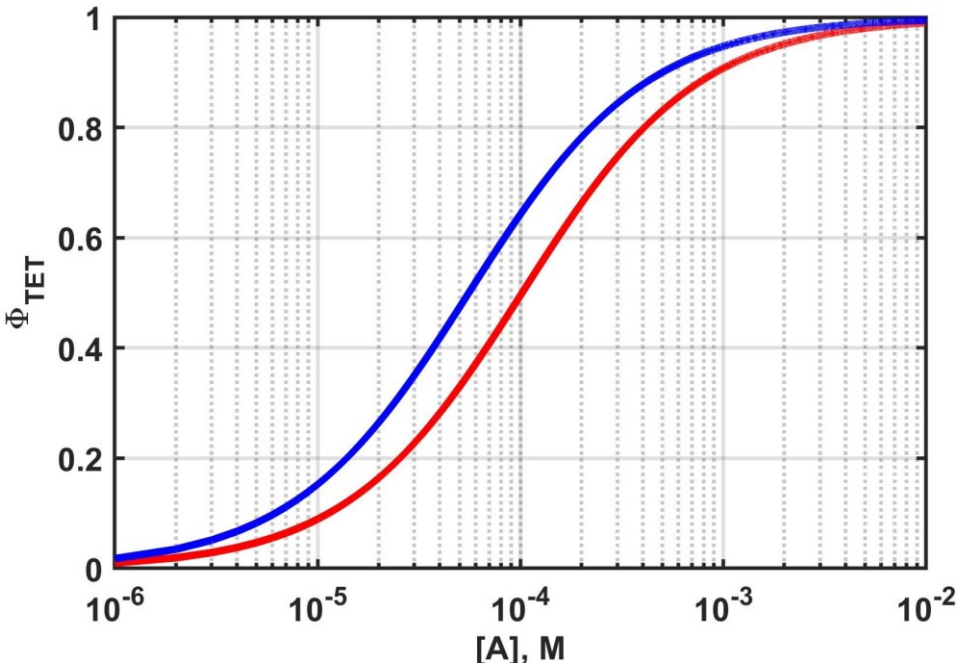

Figure 7. *Triplet-triplet energy transfer efficiencies (Φ_{TET}) of two different systems plotted against annihilator concentration ($[A]$): Exothermic case (red), where $k_{TET} = 9{,}8 \times 10^7$ ($\Delta E_T = -4\ k_B T$) and $\tau_0 = 100\ \mu s$ and endothermic case (blue), where $k_{TET} = 1{,}8 \times 10^6$ ($\Delta E_T = 4\ k_B T$) and $\tau_0 = 10\ ms$.*

Thus, by examining Eq. 16 (and Figure 7), we can conclude that higher sensitizer lifetime is beneficial for efficient TET and can promote feasible energy transfer even in endothermic cases. By using longer living sensitizer, lower annihilator concentrations can be used to achieve efficient TET, which is desirable since higher [A] can lead to aggregates or excimer formation. [69,70] Also, high [A] for efficient TET can be challenging to reach in soft matter systems, such as liposomes [35,36,71,72], polymersomes [73] and micelles [74].

2.3 Triplet-triplet annihilation

After yielding a triplet excited annihilator molecule via TET, the excited state can decay 1) non-radiatively, 2) through phosphorescence or, after collision of two annihilator molecules at their excited triplet states, 3) through triplet-triplet annihilation (TTA) [2,11,75,76]. As the triplet excited molecules collide, they form an encounter complex of singlet, triplet or quintet (Q) multiplicity as a result from the tensor product of the initial spin states. [77] Based on this tensor product, the probabilities of singlet, triplet or quintet state formation are 1/9, 3/9 and 5/9, respectively. [78–80] The encounter complex then dissociates back to its molecular species yielding [81]

$$T_1 + T_1 \xrightarrow[complex\ formation]{} [T_1 \cdots T_1] \xrightarrow[complex\ dissociation]{} \begin{cases} Q_1 + S_0 \\ T_2 + S_0 \\ S_1 + S_0 \end{cases}. \tag{17}$$

Quintet state would require two-electron excitation and is energetically unreachable [82], thus its formation can be omitted from the statistics so that the probabilities of yielding a singlet state or triplet are 1/4 and 3/4, respectively. [80,81] This distribution between the second excited triplet state (T_2) and excited singlet state is, naturally, applicable only if $E(T_2) < 2E(T_1) + k_BT$. Molecules at T_2 will rapidly convert to T_1 (through internal conversion) and are "recycled" in the TTA process to increase the singlet yield from 1/4 to 2/5. This final or total probability of yielding a singlet state via TTA is so-called spin-statistical factor f. In case of $E(T_2) > 2E(T_1) + k_BT$, the singlet yield or f will be 1. This interplay of energies is further elucidated in Figure 8.

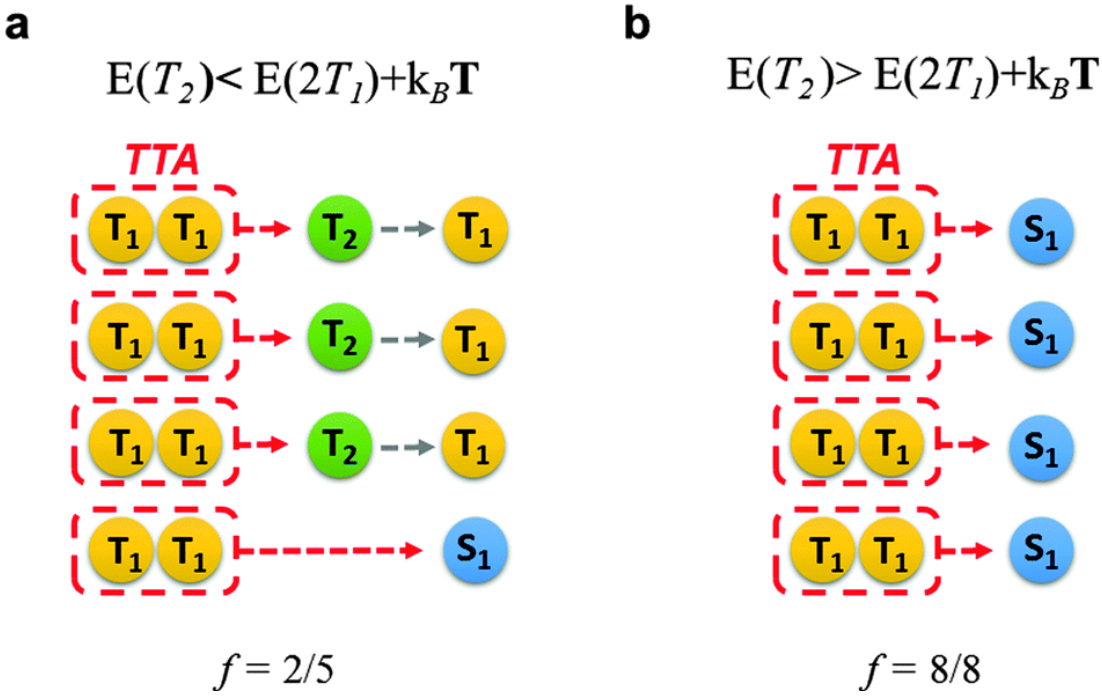

Figure 8. *The role of relative triplet energies to yield an excited singlet state upon TTA. In case* ***a*** *TTA annihilates five triplets out of eight but only two of these triplets give a singlet resulting in f = 2/5. Reproduced from Ref.* [81] *with permission from the PCCP Owner Societies.*

The energies discussed here are typically based on relaxed geometries of the annihilator molecules. Gray et al. have shown that annihilator molecules (see for example Figure 9) with conformational flexibility have a distribution of singlet and triplet energies based on the rotation angle of phenyl moieties. [83] Thus, the energy difference between singlet and triplet states changes as the rotation angle changes (since the singlet and triplet energies respond slightly differently to changes in molecular geometry), leading to a discrepancy between the singlet and triplet energy surfaces and possibly affecting the singlet state yield upon TTA. Since the rotation of the moieties depends on the viscosity of the environment [84], the singlet state yield might also differ between solvents of different viscosities thus possibly explaining the quite pronounced difference in singlet

state yield of the molecule 9,10-bis(phenylethynyl)anthracene (BPEA, see Figure 9) in low viscosity solvents (less than 5 %) [85–87] and high viscosity solvent, such as poly(ethylene glycol) (15,5 %) [61]. It is also worth mentioning, that these conformation induced effects on triplet energies may affect the efficiency of TET when the triplet energy gap is small.

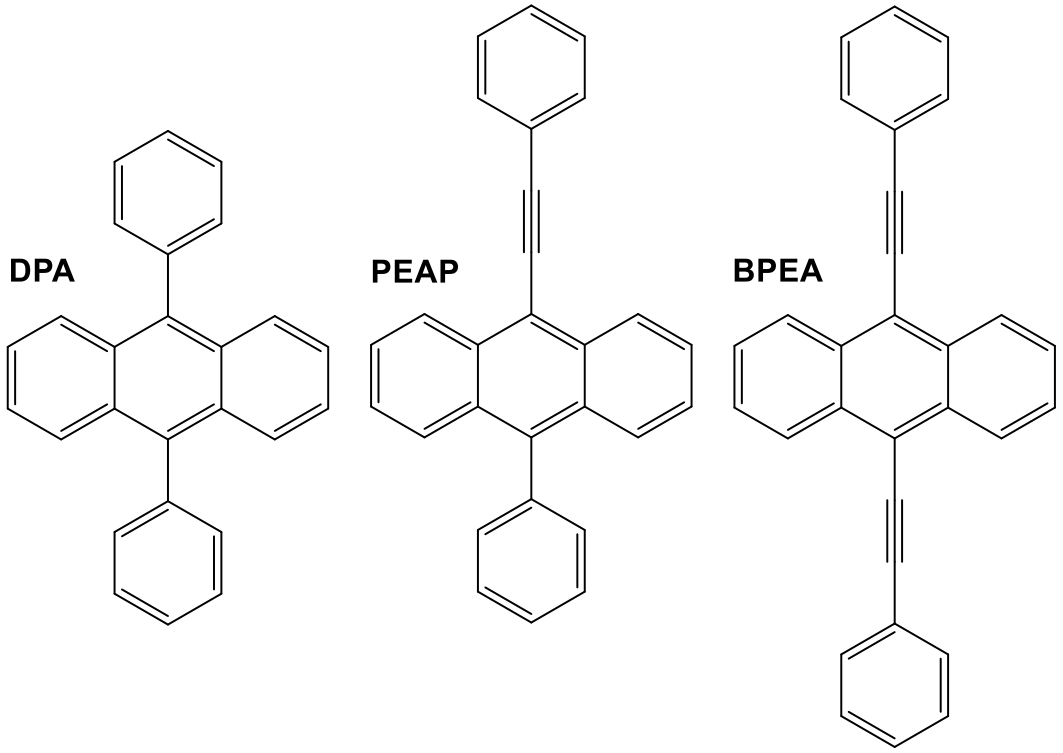

Figure 9. *Annihilator molecules possessing rotating moieties. DPA stands for 9,10-diphenylanthracene, PEAP stands for 9-(4-phenylethynyl)-10-phenylanthracene and BPEA stands for 9,10-bis(phenylethynyl)anthracene. Anthracene derivatives are generally typical annihilators.*

Kinetically, the observable rate of TTA is, as was the case with TET, ultimately decided by the rate of collisions between triplet excited annihilator molecules, which are inherently diffusion-controlled. Thus, considering that successful TTA eliminates two triplets the rate constant of TTA must be $k_{TTA} < \frac{1}{2}k_{diff}$.[b] The inequality results from limiting factors discussed next and in the beginning of this chapter.

The singlet state formed upon collision can be defined in a Cartesian coordinate system with the orientations of the molecules colliding [88]:

$$|S\rangle = \frac{|xx\rangle+|yy\rangle+|zz\rangle}{\sqrt{3}}. \qquad (18)$$

[b] This inequation can also be corroborated with Eq. 11 by regarding TTA as an energy transfer reaction where $\Delta E_T = 0 \Rightarrow k_{TTA} < k_{diff}\frac{1}{1+e^0} = \frac{1}{2}k_{diff}$.

The singlet character S of this pair is then given by the square of the projection of the pair onto the singlet state $|S\rangle$ [88]:

$$S = |\langle S|\alpha\beta\rangle|^2 = \frac{1}{3}\cos^2\theta_{\alpha\beta}, \quad (19)$$

where α and β span the axes x, y and z of the molecules colliding and $\theta_{\alpha\beta}$ is the angle between the axes defining the spin states of the molecules. Thus, we arrive to the (trivial) conclusion that $S_{maximum} = \frac{1}{3}$. This is merely a purely theoretical approach to a completely random system and it is possible that the colliding molecules are capable of orienting themselves when forming the encounter complexes [88]. Long lifetime of the triplet state may facilitate multiple encounters for each annihilator molecule thus increasing the probability of successful TTA. [77,89] The effect of annihilator triplet state lifetime on quantum yield of TTA is discussed in chapter 3.1.

2.4 Anti-Stokes fluorescence

In most cases of fluorescence (first described by Bernardino de Sahagún in 1560 and by Nicolás Monardes [90] in 1565) loss of energy occurs between excitation and emission. This energy shift caused by vibrational relaxation of the electronic states involved and solvent reorganization is called the Stokes shift after Sir G. G. Stokes's ground-breaking work [91] in the field of fluorescence. Stokes shift is generally observed with all fluorescent emitters and is experimentally defined as wavelength or frequency difference of the absorption and fluorescence spectral maxima. Intuitively, the opposite effect of emission having higher energy than the absorbed light is called anti-Stokes fluorescence [92] and often maximizing this anti-Stokes shift is desirable for a TTAUC system.

For TTAUC systems other terms, such as upconversion energy shift (UES) [83] and upconversion energy margin [67], have also been used in addition to anti-Stokes shift to describe the difference in absorbed and emitted photon energies. Typically, reported UES have been defined as the difference in energy between the blue-most emission peak of the annihilator and absorption maximum (the Q band maximum in case of porphyrins) of the sensitizer or excitation light wavelength although another definition based on intensity weighted averages of emission and absorption spectra has been suggested [18] to make comparison of different systems more standardized.

The range or extent of UES is governed, inherently, by excitation and emission photon energy and the enthalpic losses (driving forces) occurring at each step of the TTAUC process (see Figure 10) described before. The range of UES could therefore be described as a compromise between the maximum range and thermodynamic

expediency. As far as the author knows, the largest upconversion energy shifts reported have been 0,94 eV (or roughly from 660 nm to 450 nm), a value that has been reached either via entropically driven TET [67] or utilizing a fluorescein-derivative sensitizer with small energy gap between excited singlet and triplet state to minimize energy loss in ISC [93].

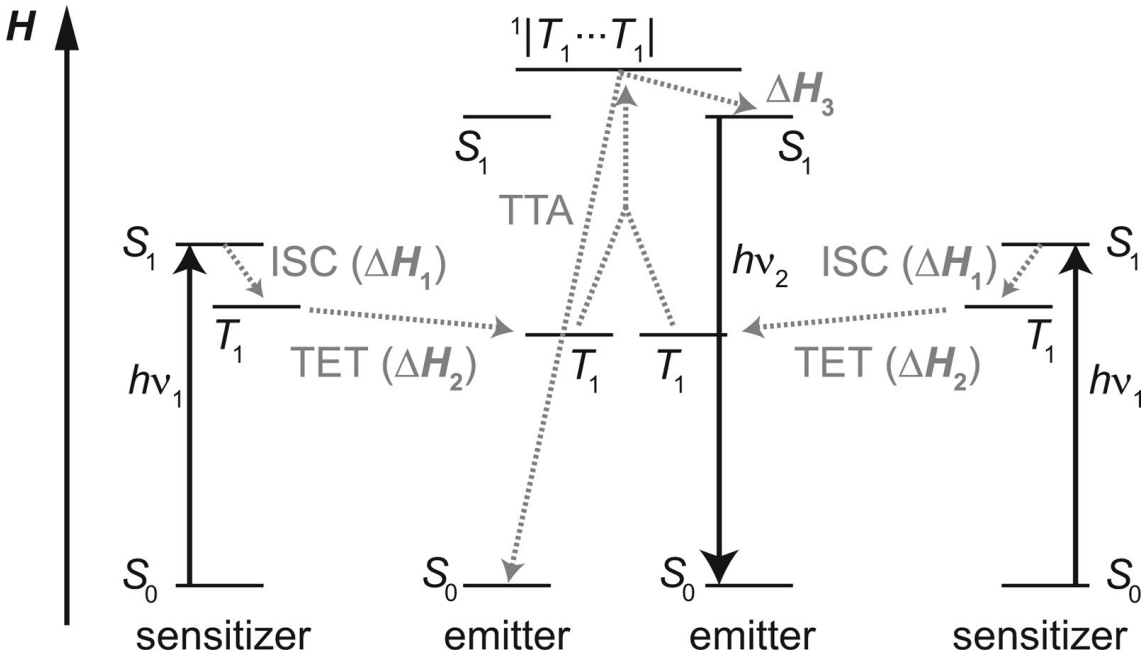

Figure 10. *The enthalpic losses involved in TTAUC. ΔH_1 is the energy difference involved in ISC, ΔH_2 is the typical enthalpic driving force of TET and ΔH_3 is the energy spent in internal conversion before annihilator fluorescence. NB the use of the term emitter in lieu of annihilator. Reprinted with permission from* [67]*. Copyright (2011) American Chemical Society.*

2.5 Oxygen and TTAUC

As already mentioned in previous chapters, an excited state can decay or deactivate via various mechanisms, but the sensitivity of the whole TTAUC process to molecular oxygen (O_2) has not been addressed yet. The ground state of O_2 is a triplet (resulting from the highest occupied molecular orbitals of O_2 being π^* and occupied by two electrons) and thus O_2 can react with either the sensitizer or annihilator when they are at their excited triplet states to produce singlet oxygen (via TTA [94]). This is harmful to the TTAUC process for two reasons which we will discuss next along with strategies to minimize the effects of O_2.

The transition $^3O_2 \rightarrow {}^1O_2$ has quite low energy of 0,98 eV (1270 nm, based on the phosphorescence of O_2) and thus ground state oxygen can effectively quench the triplet states of S and A, reducing their concentrations and hindering the TTAUC process. This

oxygen quenching pathway competes with TET and TTA and may be more efficient since it is truly diffusion controlled [95]. In addition, the atmospheric abundance of O_2 ensures that its concentration at ambient in organic solvents is typically in the order of 10^{-3} M [95] facilitating fast energy transfer from S and A triplet states. The most straight-forward method for preventing oxygen quenching is thus removing O_2 from the system before irradiation. This can be achieved by either bubbling (also called sparging or purging) the solvent with an inert gas such as helium, nitrogen or argon or by degassing the solvent with a so-called freeze-pump-thaw cycling. Another method for reducing oxygen quenching is to prevent diffusion of O_2 into the TTAUC system by using solvents with low permeability to oxygen, such as poly(ethylene glycols) [61], or utilizing physical barriers by encapsulating the TTAUC system into a matrix (e.g. a polymer film [96–98] or nano- and microstructures [33,99]) that obstructs the diffusion of O_2. This, naturally, also hinders the diffusion of the S and A molecules decreasing the TTAUC efficiency of the system. [94]

The second detrimental aspect of O_2 is the increased reactivity of singlet oxygen that can photodamage the chromophores or the matrix. [94] In biological application singlet oxygen can cause cell and tissue damage, an effect exploited in photodynamic therapy of cancer. [100] The effects of singlet oxygen can be mitigated by employing oxygen scavengers, reducing agents acting as antioxidants, that react rapidly with singlet oxygen upon irradiation of the TTAUC system. [94] Examples of oxygen scavengers are polyphosphates [101], polyisobutylene [102], oleic acid [32,61], sulfite, ascorbate, glutathionate, L-histidine and trolox [73]. By utilizing oxygen scavengers, two goals can be achieved: the chromophores are protected from photodamage and upon irradiation molecular oxygen is depleted (locally at the site of irradiation) from the system enhancing the efficiency of TTAUC. [94]

3. MAXIMIZING THE EFFICIENCY OF TTAUC

In addition to the upconversion energy shift discussed earlier, two other parameters have become figures of merit for evaluating TTAUC systems: the quantum yield of upconversion [18] and the power density (intensity) threshold [77]. An efficient TTAUC system in the context of this work is thus, defined with these parameters, capable of upconverting low intensity light with high quantum yield.

3.1 Quantum yield of upconversion

Quantum yield (Φ) of a general photochemical process is defined as [95]

$$\Phi = \frac{Number\ of\ given\ species\ formed}{Number\ of\ photons\ absorbed}. \quad (20)$$

The absolute quantum yield is given by the product of the quantum yields or efficiencies of the individual processes involved in the process. [95] For TTAUC the absolute quantum yield is thus [3]

$$\Phi_{UC} = \frac{1}{2} f \Phi_{ISC} \Phi_{TET} \Phi_{TTA} \Phi_{fluo}, \quad (21)$$

where factor $\frac{1}{2}$ comes from the fact that two low-energy photons are needed to yield one high-energy one, f is the spin statistical factor discussed in ch. 2.3, Φ_{ISC} is the quantum yield of ISC, Φ_{TET} is the quantum yield or efficiency of TET (see Eqs. 15 and 16), Φ_{TTA} is the quantum yield of TTA and Φ_{fluo} is the quantum yield of annihilator fluorescence.

Φ_{TTA} depends on the kinetics of the system and since the states involved in TTA are products of the preceding processes, Φ_{TTA} can be expressed as [77]

$$\Phi_{TTA} = \frac{k_{TTA}}{k_{tot}^{T_A}} = \frac{\gamma_{TT} T_A}{k_{tot}^{T_A}} = \frac{\gamma_{TT}(\Phi_{ISC}\Phi_{TET}\alpha(E) I_{exc})}{\left(k_{tot}^{T_A}\right)^2}, \quad (22)$$

where k_{TTA} is the rate of TTA, $k_{tot}^{T_A}$ is the total decay rate of annihilator triplet state, γ_{TT} is the second-order decay rate of TTA in $cm^{-3}s^{-1}$ [103], T_A is the population of annihilator triplet states, $\alpha(E)$ is the absorption coefficient of sensitizer in cm^{-1} and I_{exc} is the excitation intensity in $\frac{photons}{s\ cm^2}$.

Notably, the quantum yield is decided by both intrinsic photophysical properties of the sensitizer and annihilator and their concentrations. For example, Φ_{ISC}, f and Φ_{fluo} depend on the intrinsic properties of the molecules. Φ_{TET} depends on the energy gap

(intrinsic for A and S) and the concentration of A (see Eq. 16). Φ_{TTA} depends on the other hand on both properties and concentrations of the molecules (see Eq. 22). Strictly, Φ_{fluo} also depends on A concentration, since the typically high concentrations utilized in TTAUC lead to fluorescence quenching by excimer formation and aggregation. [81,104]

To retain high Φ_{TTA} and subsequently high Φ_{UC} at lower excitation intensities, high absorption ($\alpha(E)$) is required (see Eq. 22). This can be addressed by using a sensitizer with high molar extinction coefficient at the excitation wavelength (range) and using sufficiently high concentration. Here the use of the word sufficient is deliberate to indicate certain ambiguity, since the optimal concentration depends on variety of parameters: in some cases high concentration of sensitizer can lead to RTET (see Eq. 13), quench annihilator triplet state [105] and cause other issues discussed in the next chapter.

3.2 Power density threshold

The kinetics of a TTAUC system can be depicted by using a set of coupled equations: [77]

$$\frac{\partial T_S}{\partial t} = \alpha(E) I_{exc} \Phi_{ISC} - k_0^{T_S} T_S - k_{TET} T_S + k_{RTET} T_A \quad (22a)$$

$$\frac{\partial T_A}{\partial t} = k_{TET} T_S - k_0^{T_A} T_A - k_{RTET} T_A - \gamma_{TT} T_A^2 \quad (22b)$$

$$\frac{\partial S_A}{\partial t} = \frac{1}{2} f \gamma_{TT} T_A^2 - k_0^{S_A} S_A, \quad (22c)$$

where $k_0^{T_S}$ is the spontaneous decay (phosphorescence and non-radiative) rate of sensitizer triplet state, T_S is the sensitizer triplet state population, T_A is the annihilator triplet state population, $k_0^{T_A}$ is the spontaneous decay rate of annihilator triplet state, S_A is the annihilator singlet state population and $k_0^{S_A}$ is the decay rate (fluorescence and non-radiative).

For steady-state conditions (with continuous excitation $\frac{\partial T_S}{\partial t} = \frac{\partial T_A}{\partial t} = \frac{\partial S_A}{\partial t} = 0$), Eq. 22 can be solved. Let us now focus on two cases: fast or strong and slow or weak annihilation limits. In the strong annihilation limit, TTA is more probable than the spontaneous decay of annihilator triplet state, namely $\gamma_{TT} T_A^2 \gg k_0^{T_A} T_A$, which is expected at high excitation intensity promoting large T_A. Thus, when solving Eq. 22, term $k_0^{T_A} T_A$ is neglected (as well as terms regarding RTET for the sake of simplicity) resulting in [106]

$$S_A = \frac{1}{2} f \frac{1}{k_0^{S_A}} \left[\frac{k_{TET}}{k_0^{T_S} + k_{TET}} \right] \Phi_{ISC} \alpha(E) I_{exc}. \quad (23)$$

The most important aspects of Eq. 23 are the linear dependency of S_A (and thus upconverted fluorescence intensity) and I_{exc} and the non-dependency between S_A and γ_{TT}. The linear relation between S_A and I_{exc} manifests itself when upconverted fluorescence intensity is plotted against the excitation intensity in a double logarithmic plot resulting in a slope of 1.

Accordingly, in the weak annihilation limit the spontaneous decay is the main deactivation channel of T_A ($k_0^{T_A} T_A \gg \gamma_{TT} T_A^2$). Again, solving Eq. 22 (neglecting terms of RTET) yields then [106]

$$S_A = \frac{1}{2} f \frac{\gamma_{TT}}{k_0^{S_A}} \left[\frac{k_{TET}/k_0^{T_A}}{k_0^{T_S} + k_{TET}} \right] [\Phi_{ISC} \alpha(E) I_{exc}]^2. \tag{24}$$

The most notable result of Eq. 24 is the quadratic relation between S_A and I_{exc} resulting in a slope of 2 in a double logarithmic plot.

Now, after defining the weak and strong annihilation limits, we can consider the interesting case of I_{exc} at which the TTA and spontaneous decay of T_A contribute equally ($k_0^{T_A} T_A = \gamma_{TT} T_A^2$). Thus, by equating Eqs. 23 and 24 we can define the so called intensity or power density threshold I_{th} [77] in photon rate ($photons\ s^{-1} cm^{-2}$):

$$I_{th} = \frac{2\left(k_0^{T_A}\right)^2}{\alpha(E) \gamma_{TT} \Phi_{TET}}. \tag{25}$$

The term threshold stems from the fact that at $I_{exc} > I_{th}$ TTA is the main deactivation channel of annihilator triplet states and respectively at $I_{exc} < I_{th}$ the excitation energy is mostly consumed in spontaneous decay thus resulting in inefficient upconversion. We also arrive at the conclusion that $\Phi_{TTA} = 0{,}5$ at I_{th}. [77] By studying Eq. 25, we can deduce that I_{th} can be lowered by using annihilator with long triplet lifetime ($k_0^{T_A} = 1/\tau$) or increasing sensitizer absorption coefficient which also compensates for lower I_{exc} in quantum yield (see previous chapter and Eq. 22).

Durandin et al. have explored the effect of sensitizer properties (molar extinction coefficient at excitation wavelength, triplet state lifetime and energy) on I_{th}. [107] Through experimental studies and kinetic rate modelling they have demonstrated that once the energy gap between sensitizer and annihilator triplet states begins to diminish, the sensitizer triplet state lifetime starts to determine the I_{th} for the system and an optimum (in terms of I_{th}) sensitizer ground state concentration can be found for a given system (see Figure 11). The overall effect of the energy gap on I_{th} with different annihilator ground state concentrations was also studied. These results are shown in Figure 12.

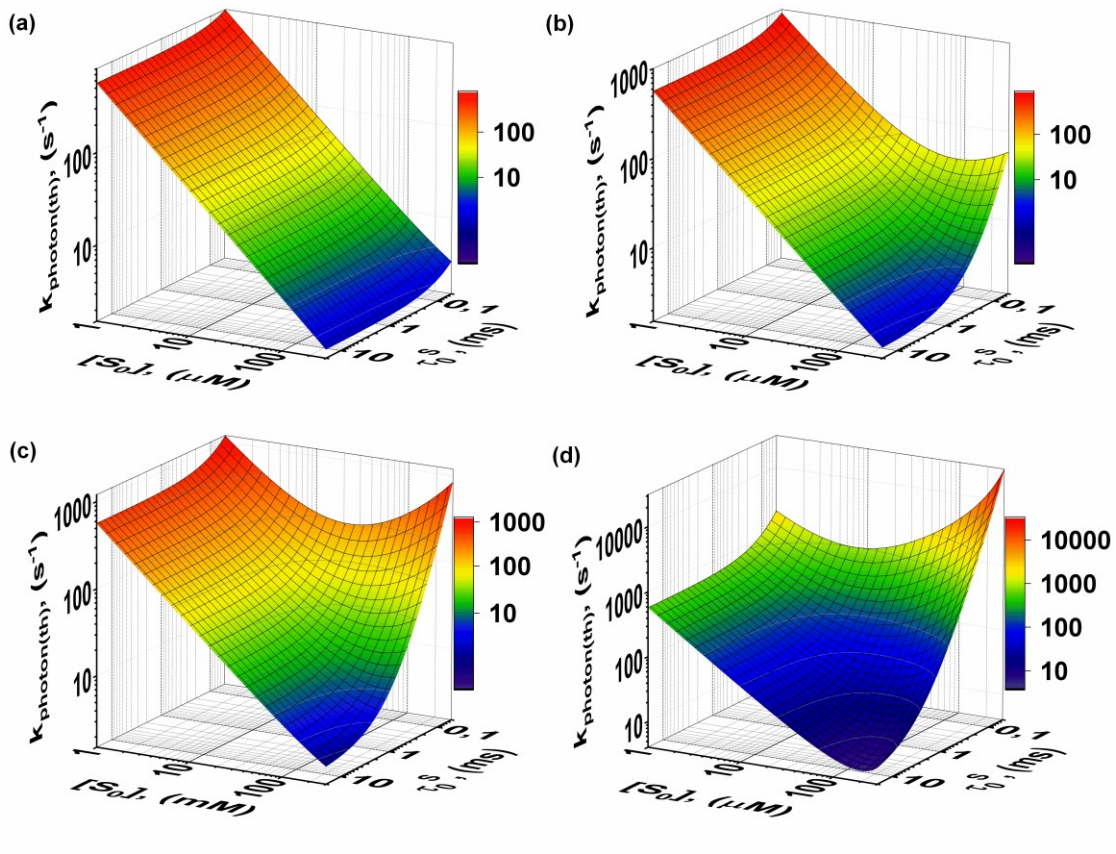

Figure 11. *The power density threshold of a TTAUC system in photon rate ($k_{photon(th)} = I_{th}$ in 1 cm^2) as a function of sensitizer ground state concentration ($[S_0]$) and sensitizer triplet state lifetime (τ_0^S). The annihilator ground state concentration is constant 3 mM. The energy gap between the sensitizer and annihilator is 4 k_BT* ***(a)****, 1 k_BT* ***(b)****, 0 k_BT* ***(c)*** *and -0,8 k_BT* ***(d)****. At shorter triplet state lifetimes the parabolic behaviour of I_{th} starts to manifest when the energy gap becomes smaller. Figure is based on the modelling results presented in* [107].

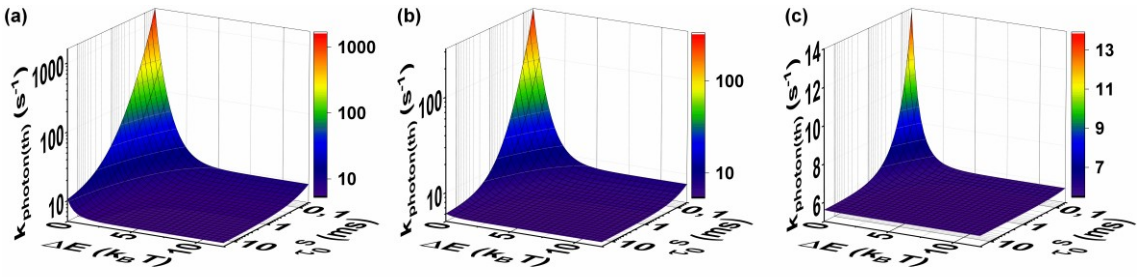

Figure 12. *The power threshold of a TTAUC system in photon rate ($k_{photon(th)}$) as a function of energy gap between sensitizer and annihilator (ΔE) and sensitizer triplet state lifetime (τ_0^S) at a constant sensitizer concentration of 100 μM. The annihilator ground state concentrations are 0,5 mM* ***(a)****, 3 mM* ***(b)*** *and 30 mM* ***(c)****. NB the sign of ΔE is opposite to the definition of ch. 2.2 (here positive value means exothermic) and the z-axes are logarithmic in* ***(a)*** *and* ***(b)*** *while linear in* ***(c)****. Figure is based on the modelling results presented in* [107].

The behaviour presented in both Figures 11 and 12 can principally be explained by RTET. Initially increasing sensitizer concentration reduces I_{th} by increasing triplet state generation of sensitizer and consequently annihilator triplet states. However, most notably at shorter sensitizer lifetimes and smaller energy gaps, overly large sensitizer concentration leads to RTET that quenches annihilator triplet states ($k_0^{T_A}$ becomes larger, see Eq. 25) and results in larger I_{th}. Figure 12 shows how RTET can be effectively suppressed by increasing annihilator concentration and utilizing a sensitizer with longer living triplet state leading to smaller I_{th}. This supressing of RTET can ultimately be explained with Eq. 13: the entropy change involved in TET increases with higher annihilator concentration and longer triplet state lifetime of sensitizer (which means that at any given time S triplet state population is larger). Conclusively, long sensitizer triplet state lifetime is decidedly beneficial for TTAUC systems. A long living sensitizer can even render a TTAUC system with endothermic TET efficient. Finally, large molar extinction coefficient is highly desirable for a sensitizer since high absorption can be attained without exceedingly high sensitizer concentrations. [107]

3.3 Requirements for sensitizer and annihilator

We have already discussed most of the specifications necessary for an efficient TTAUC system. To conclude this review, a list of requirements for the active molecules is presented: [3,15]

For sensitizer:

- Strong absorption (high molar extinction coefficient) in the desired wavelength range
- High quantum yield of intersystem crossing
- Long triplet state lifetime (>10 μs) for efficient TET
- Small singlet-triplet gap to maximize upconversion energy shift[c]

For annihilator:

- A long triplet state lifetime (> 100 μs) for efficient TTA
- High fluorescence quantum yield
- $E(S_1) < 2E(T_1) < E(T_2)$ to maximize singlet yield upon TTA

A typical sensitizer is a Pd and Pt coordinated porphyrins due to their high intersystem crossing efficiency ($\Phi_{ISC} \approx 1$ due to heavy atom effect) and low energy Q band absorption. [16,108] Zn coordinating porphyrins have also been utilized in efficient

[c] However, triplet-triplet gap should be >1 k_BT to prevent reverse ISC resulting in thermally activated delayed fluorescence (TADF) [129] and reduced sensitizer triplet population.

TTAUC despite of non-unity Φ_{ISC}. [83,104] Metallated phthalocyanines, molecules closely related to porphyrins by structure and photophysical properties, are also capable sensitizers [109–112], although less employed than porphyrins possibly due to poor solubility [113]. Other transition metal complexes, such as $Ir(ppy)_3$ [70] and $Ru(dmb)_3$ [114], have been used to sensitize TTAUC. Metal and other heavy atom-free sensitizers are rare, but one interesting group of molecules is so-called Bodipys that are able to sensitize TTAUC. [115–118]

Compared to sensitizers, there is less variety among annihilators, possibly due to the quite strict requirements regarding the singlet and triplet energy levels while expressing high fluorescence quantum yield. The most typical annihilators are polyaromatic hydrocarbons, such as derivatives of anthracene (see Figure 9), perylene and rubrene. [15,108]. Use of other type of molecules remains scarce (only two studies using bodipys [119] or a bodipy-perylene compound [120]) since most studies utilize commercially available molecules and only limited effort has been put into designing new annihilators. [16]

4. EXPERIMENTAL METHODS

The experimental part of this work consisted of basic photophysical characterization (steady state absorption and photoluminescence and phosphorescence lifetime) of two porphyrins, PdTAPIP and ZnTAPIP (TAPIP = tetraarylphtalimidoporphyrin or N-{2,6-di[(3'(methoxycarbonyl)propyloxy)phenyl]} phthalimido-porphyrin) and one anthracene derivative, PEAP (9-phenyl-10-(phenylethynyl)anthracene), and their utilization in triplet-triplet annihilation upconversion. The molecular structures of these molecules are shown in Figure 13. The performance of both porphyrins as sensitizers and PEAP as annihilator for TTAUC was evaluated by annihilator titration and determining the upconversion quantum yields and power density thresholds in two viscous systems using either PEG200 (poly(ethylene glycol), average molecular mass of 200 g/mol) at room temperature or PEG300 (poly(ethylene glycol), molecular mass of 285–315 g/mol) at -5 ℃. At this temperature PEG300 still remains liquid while its viscosity increases substantially.

The porphyrins were provided by professor Sergei Vinogradov (University of Pennsylvania). The synthesis and characterization of these porphyrins is described in [121]. PEAP was provided by Dr. Alexander Efimov (Tampere University). The synthesis of PEAP is described in [83]. Other materials were obtained from commercial sources and used as received.

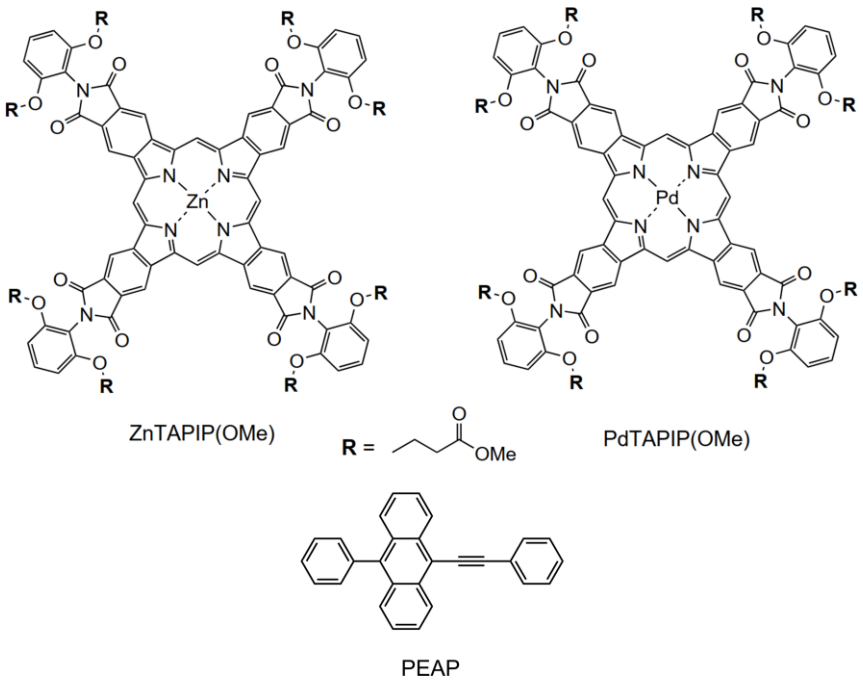

Figure 13. *The molecular structures of ZnTAPIP, PdTAPIP and PEAP.*

4.1 Steady state photophysical characterization

Absorption measurements were performed using a Shimadzu UV-3600 UV-Vis-NIR Spectrophotometer. The absorption spectra of PdTAPIP, ZnTAPIP and PEAP were measured in dichloromethane (DCM), PEG200 and PEG300. The molar exctinction coefficients of PEAP was determined in both DCM and PEG200 by measuring the absorbance of PEAP at four different concentrations in both solvents and obtaining the slope of their linear fit. The molar extinction coefficients of the porphyrins were provided by prof. Vinogradov.

The steady state photoluminescence (prompt fluorescence and phosphorescence) spectra of PEAP and the porphyrins were measured in both DCM and PEG200 with Edinburgh Instruments FLS1000 Photoluminescence Spectrometer equipped with excitation and emission double monochromators and PMT-900 photomultiplier tube detector. The excitation source was a 450 W xenon arc lamp. The samples were prepared so that maximum absorbance was less than 0,1 to minimize inner filter effect, aggregation and excimer formation. For phosphorescence measurements in PEG200 the samples were bubbled rigorously with nitrogen for an hour.

4.2 Phosphorescence lifetime and quenching

The phosphorescence decays of PdTAPIP and ZnTAPIP were recorded with Edinburgh Instruments FLS1000 Photoluminescence Spectrometer using a microsecond flashlamp as an excitation source. The phosphorescence lifetimes were obtained from the decays by monoexponential fitting in the Fluoracle program (Edinburgh Instruments). The phosphorescence lifetimes were determined in both viscous systems. The samples were prepared so that absorbance was 0,1 at the Q band maximum of both porphyrins (serving as the excitation wavelength) and bubbled with nitrogen for an hour prior to measuring.

The Stern-Volmer constants (and consequently TET rate constants) of the porphyrins and PEAP were determined by phosphorescence lifetime measurements with increasing PEAP concentrations in both viscous systems. PEAP was added as DCM solution to the samples and after each addition the samples were bubbled with nitrogen for at least half an hour before measuring the phosphorescence lifetime. All phosphorescence samples were prepared in a SOG9 flash cuvette sealed with a silicon rubber/PTFE septum. The Stern-Volmer constants were determined by plotting the ratio of unquenched phosphorescence lifetime and quenched lifetime at corresponding annihilator concentration and fitting a linear function (in Origin 2017) with a set intercept of 1 at zero concentration.

4.3 Upconversion power threshold and annihilator titration

The scheme of the experiment setup for determining the power density thresholds for both porphyrins in both viscous systems is shown in Figure 14. The samples were prepared as follows: 1,25 ml of either PEG200 or PEG300 was added into a SOG9 flash cuvette. 60 µl of oleic acid (OA) was added into the cuvette. The concentration of porphyrin was chosen so that the absorbance at the excitation wavelength (633 nm for PdTAPIP and 660 nm for ZnTAPIP) was 1 (in PEG200) or 2 (in PEG300). The porphyrin was added as DCM solution into the sample and the absorbance was measured with a Shimadzu UV-3600 UV-Vis-NIR Spectrophotometer. PEAP was added either as a 10 mM or 20 mM DCM solution into the sample. Finally, the sample was bubbled with nitrogen for at least two hours to remove DCM and dissolved oxygen from the sample before measurements. The cuvette was sealed with a silicon rubber/PTFE septum. In case of annihilator titration, the sample was bubbled for an hour after each addition of PEAP solution before measuring. The PEAP concentrations used for the power threshold measurements were based on the titration results.

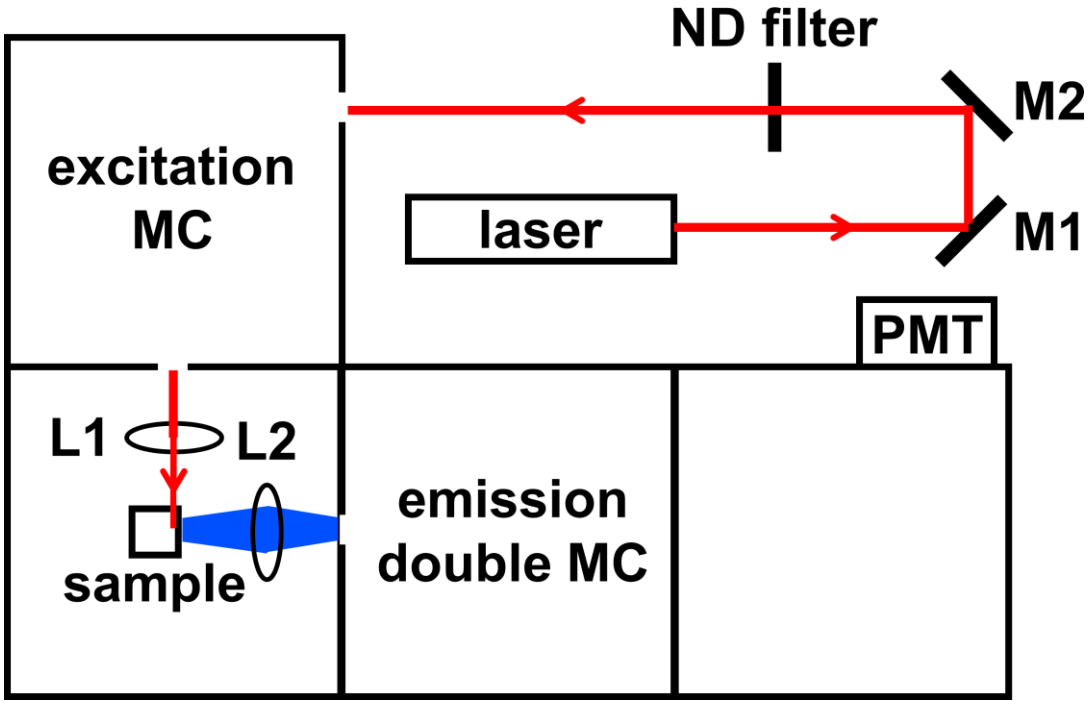

Figure 14. *The experiment setup for measuring upconversion intensity and spectrum to determine the power threshold for both porphyrins in both viscous systems. The excitation source is either a helium-neon laser or a laser diode. M1 and M2 are adjustable mirrors for beam alignment. ND (neutral density) filters were used to attenuate the excitation power. The excitation beam was directed through a monochromator (MC) to the sample chamber were the beam size was adjusted with a convex lens (L1). The upconverted light was collected with another convex lens (L2) into a double monochromator and finally to the photomultiplier tube (PMT).*

The experiment setup utilized the detector, monochromators and sample chamber optics of the Edinburgh Instruments FLS1000 Photoluminescence Spectrometer. It is unconventional to couple a laser with a monochromator, but in this case, it enabled the use of sample chamber optics to adjust the laser beam size. The excitation source for PdTAPIP was a helium-neon (HeNe) laser (HNL210LB, 21 mW, polarized, Thorlabs) and for ZnTAPIP a laser diode (06-MLD 660 nm, 100 mW, Cobolt). The excitation power at the sample was measured with PM100D Digital Optical Power and Energy Meter (Thorlabs) using a S120VC Si photodiode power sensor (Thorlabs). About 80 % of the laser power was lost in the excitation monochromator when using HeNe laser and 90 % when using the laser diode.

The beam profile and dimensions were measured with a LBP2-HR-VIS2 Laser Beam Profiler (Newport) and determined with LBP2 Software (Newport) and its Auto-aperture feature. The beam profiles are shown in Figure 15. The laser powers were modulated with neutral density filters (Edmund Optics) and with Cobolt Monitor Software when laser diode was used. The power densities were calculated by using the dimensions of the beam profile as the axes of an ellipse and dividing the measured power with the area of said ellipse. The beam size at the front face of the cuvette was adjustable by turning L1 and thus changing the location of its focal point.

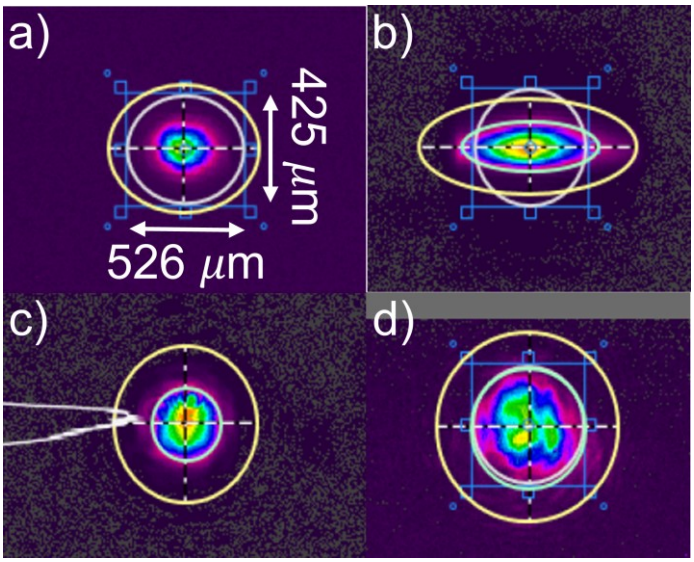

Figure 15. *The laser beam profiles. All of the subfigures are in the same scale.* ***(a)*** *HeNe laser inside the sample chamber* ***(b)*** *laser diode inside the sample chamber* ***(c)*** *HeNe laser as used in quantum yield measurements* ***(d)*** *laser diode as used in quantum yield measurements. The measurements are based on the so called second moments method* [122].

The sample holder was custom-made so that sample position was tuneable to ensure excitation right next to the cuvette wall (to minimize inner filter effect), to enable cooling of the sample (using a Huber Ministat 125 cooling circulator filled with 1:1 water/ethylene

glycol mixture) and stirring with a magnetic stirrer while measuring. When cooling was used, the sample temperature was monitored with a FLIR TG165 thermal camera. Also, the upconverted fluorescence intensity was used to verify the cooling prior to measuring since TET rate and TTA rate and thus upconversion intensity are viscosity-dependent. This meant that the upconversion intensity dropped during cooling and reached a plateau when thermal equilibrium with the sample holder was reached. During the low temperature measurements, a constant flow of nitrogen was maintained in the sample chamber to prevent condensation and formation of ice.

4.4 Upconversion quantum yield

Φ_{UC} was measured by comparing upconverted fluorescence intensity to Zn phthalocyanine (ZnPc, $\Phi_{fluo} = 0{,}2$ [123]) and methylene blue (MB, $\Phi_{fluo} = 0{,}04$ [124]) fluorescence intensities: [125]

$$\Phi_{UC} = 2\Phi_{std}\left(\frac{A_{std}}{A_{UC}}\right)\left(\frac{I_{UC}}{I_{std}}\right)\left(\frac{\eta_{UC}}{\eta_{std}}\right)^2, \quad (26)$$

where Φ_{std} is the fluorescence quantum yield of the standard, A_{std} and A_{UC} are the absorbances of the standard and the upconversion sample at the excitation wavelength, I_{UC} and I_{std} are the integrated emission intensities and η_{UC} and η_{std} are the refractive indices of the solvents used (PEG200 for upconversion samples, DMSO for ZnPc and Milli-Q water for methylene blue). The factor 2 is added to Eq. 26 since TTAUC is a two-photon process. [3] The concentrations of the standards were kept low (absorbance of 0,1 at excitation wavelength) to ensure monomeric fluorescence and to minimize inner filter effect.

The upconversion fluorescence and standard fluorescence were measured using an experiment setup based on the setup used in [104] and presented in Figure 16. In order to yield the maximum quantum yield, the power densities were kept well above the power density threshold. The quantum yield measurements were performed only using PEG200 as a solvent since the low temperature used for I_{th} measurements would have resulted in rapid formation of ice on the sample cuvette as the cuvette was not enclosed in a chamber as it was for I_{th} measurements. Thus, Φ_{UC} was estimated for the PEG300 samples as follows: The same experimental setup was used for both PEG200 and PEG300 samples for I_{th} measurements and annihilator titration, so a ratio between the emission intensities recorded with these measurements in PEG200 and PEG300 was calculated. This ratio was used directly to correlate the quantum yields measured with the standards to the quantum yields in PEG300.

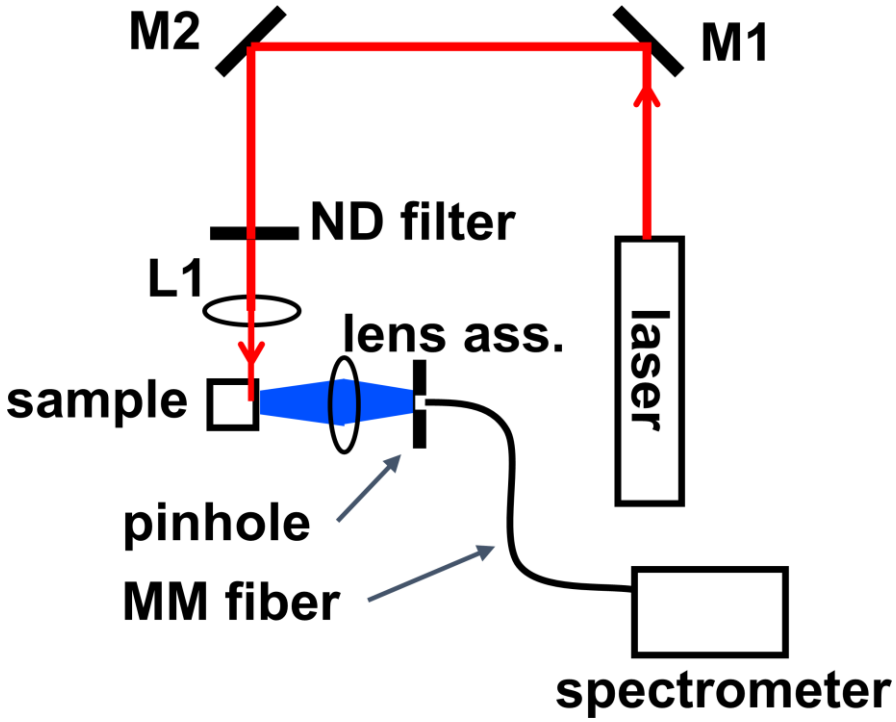

Figure 16. *The experiment scheme for measuring Φ_{UC}. Again, the mirrors M1 and M2 were used to align the laser beam, neutral density filters were used to adjust the laser power and a convex lens was used to adjust the beam size. Fluorescence was collected by using a lens assembly of two convex lenses that focused the fluorescence into an optical fiber coupler (pinhole). The fluorescence spectrum was recorded with an AvaSpec-ULS2048L (Avantes) fiber-optic spectrometer.*

The recorded spectra were corrected for inner filter effect using the monomeric fluorescence of PEAP by using so called tail fitting procedure: the fluorescence intensities were matched from 525 nm (after PEAP and porphyrin absorption) and the upconversion fluorescence intensities at the shorter wavelengths were recalculated according to the relative intensities of monomeric PEAP fluorescence. PEAP showed no excimer emission even at 20 mM concentration, so tail fitting provided a facile way to correct the spectra. The Φ_{UC} samples were prepared as explained in the previous chapter.

4.5 Viscosity measurements

The viscosities of PEG200 at room temperature and PEG300 at -5 ℃ were measured by Dr. Ilari Jönkkäri (Tampere University) using an Anton Paar MCR 301 rotational rheometer. The dynamic viscosities provided by these measurements were used to validate the results obtained from the phosphorescence quenching studies.

5. RESULTS AND DISCUSSION

5.1 Steady state photophysical characterization

The characterization of the porphyrins begun by measuring their absorption spectra in DCM and PEG200. The absorption spectra of ZnTAPIP and PdTAPIP in DCM and PEG200 are shown in Figures 17 and 18, respectively. No difference between absorption spectra in PEG200 and PEG300 was observed, meaning that maxima and absorbance were equivalent.

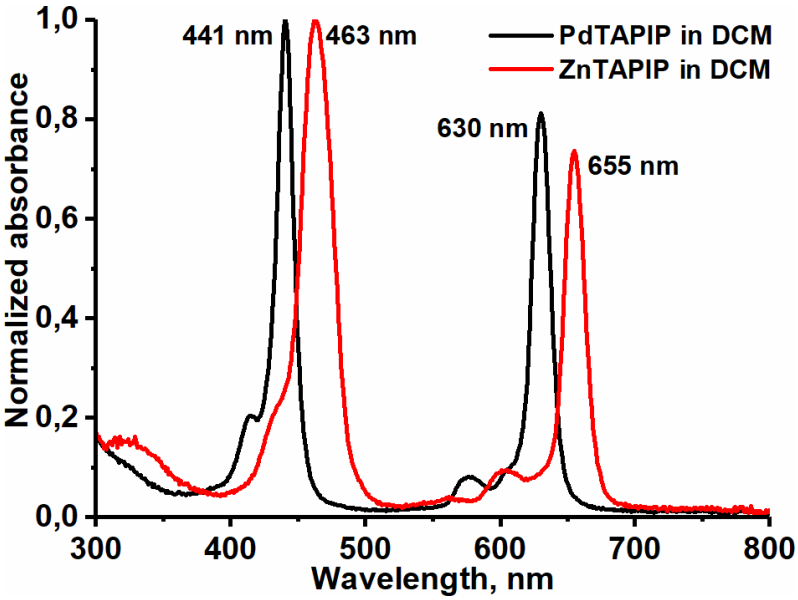

Figure 17. *Normalized absorption spectra of PdTAPIP and ZnTAPIP in DCM.*

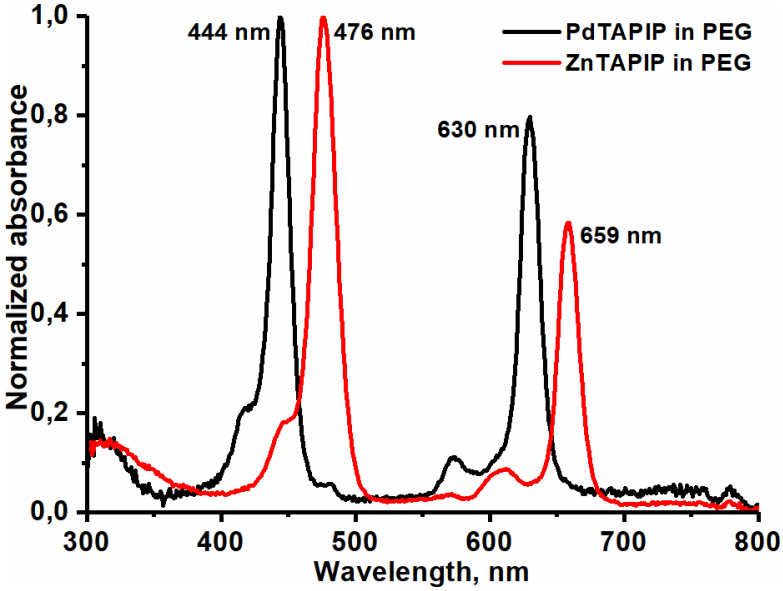

Figure 18. *Normalized absorption spectra of PdTAPIP and ZnTAPIP in PEG.*

The absorption spectra of PEAP in DCM and PEG200 are shown in Figures 19 and 20, respectively. The molar extinction coefficients of PEAP were determined by measuring its absorbance at four different concentrations. Again, no change in absorption was observed between PEG200 and PEG300.

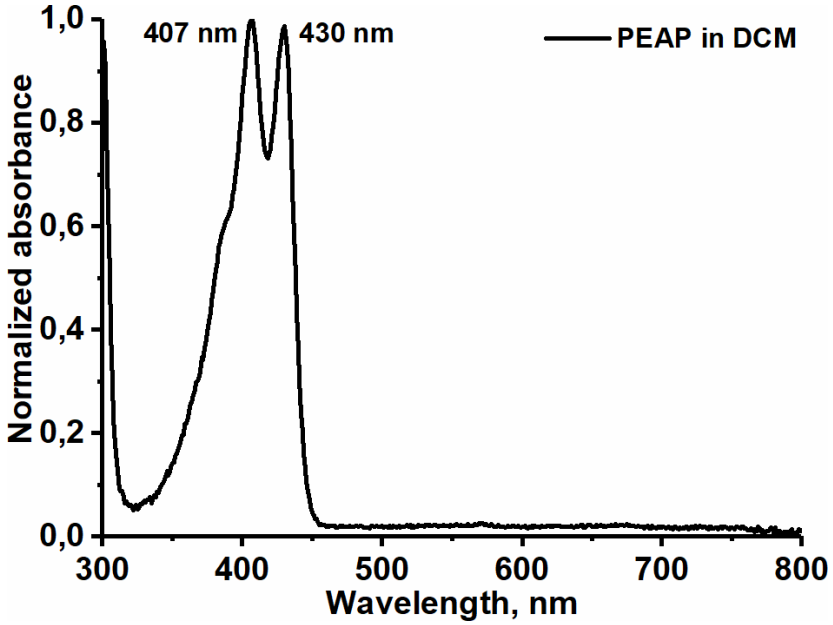

Figure 19. *Normalized absorption spectrum of PEAP in DCM.*

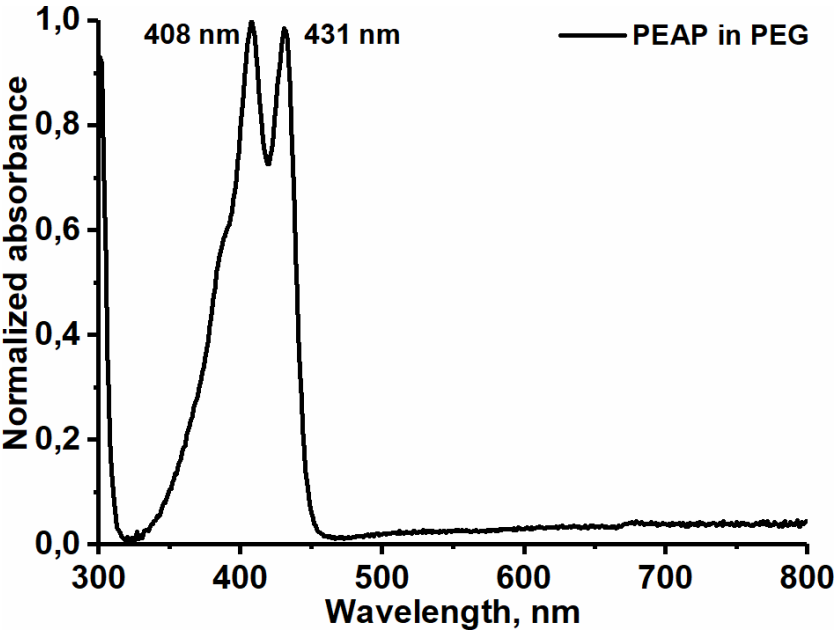

Figure 20. *Normalized absorption spectrum of PEAP in PEG200.*

NB that each spectrum has been normalized to its own maximum value. For comparison between the molecules, see the extinction coefficients of PdTAPIP, ZnTAPIP and PEAP in DCM and PEG200 in Table 1.

Table 1. *The extinction coefficients ϵ of PdTAPIP, ZnTAPIP and PEAP with respective peak wavelengths.*

	ϵ in DCM, $M^{-1}cm^{-1}$	ϵ in PEG200, $M^{-1}cm^{-1}$
PdTAPIP, 441 nm / 444 nm	342 900	342 900
PdTAPIP, 630 nm / 630 nm	263 500	263 500
ZnTAPIP, 463 nm / 476 nm	271 900	356 300
ZnTAPIP, 655 nm / 659 nm	191 200	198 500
PEAP, 407 nm / 408 nm	21 000	21 000
PEAP, 430 nm / 431 nm	20 600	20 700

By examining the molar extinction coefficients of the TAPIPs, it is evident that they are very potent dye molecules. Especially, the strong Q band absorption makes both TAPIPs attractive to utilize in TTAUC studies. The Q band peaks of both porphyrin match well with commercial laser wavelengths, helium-neon for PdTAPIP and a laser diode for ZnTAPIP.

The luminescence spectrum of PdTAPIP in N_2 bubbled PEG200 with OA added is shown in Figure 21. PdTAPIP is strongly emissive with 23 % quantum yield of phosphorescence (in DMA) and exhibits also residual and delayed fluorescence at 636 nm. [121] The high exctinction coefficients and strong luminescence make PdTAPIP appealing for other applications besides TTAUC, e.g. oxygen probing [126]. PdTAPIP has T_1 energy of 1,61 eV, determined from the phosphorescence peak.

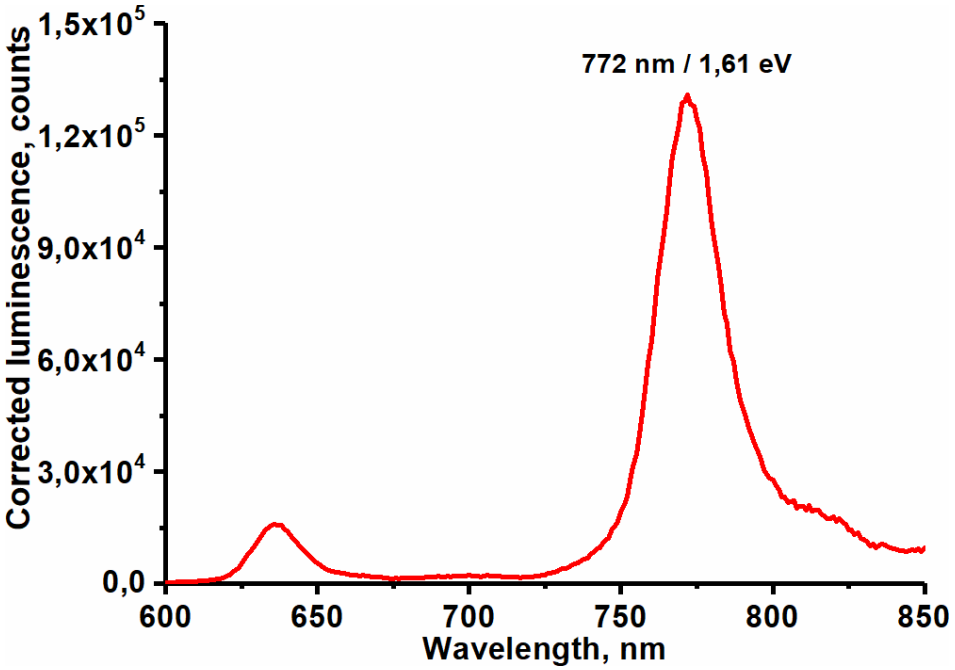

Figure 21. *Luminescence spectrum of PdTAPIP in deoxygenated PEG200 and excited with xenon lamp at 444 nm. The phosphorescence is highlighted with peak wavelength and energy.*

The luminescence spectrum of ZnTAPIP is shown in Figure 22. Since ZnTAPIP exhibits prompt fluorescence and it is partially overlapping with phosphorescence, the luminescence was recorded before and after deoxygenation (bubbling and addition of OA). Thus, a new peak appeared after deoxygenation. This peak is attributed to ZnTAPIP's phosphorescence from which the T_1 energy is determined as 1,53 eV. The fluorescence quantum yield of ZnTAPIP is 10 % (in DMA) [121]. From this the phosphorescence quantum yield of ZnTAPIP can be roughly estimated by comparing the integrated luminescence intensities: luminescence before 788 nm is attributed to fluorescence and rest for phosphorescence. Thus the quantum yield of phosphorescence is approximately 0,7 % (not taking into account the "tail" of phosphorescence beyond 850 nm).

The difference in phosphorescence quantum yield between the TAPIPs can be explained by ISC efficiencies. Pd being a heavier atom than Zn (by over 60 %), the spin-orbit coupling in PdTAPIP is stronger than in ZnTAPIP. $\Phi_{ISC}^{T_1 \leftarrow S_1}$ for PdTAPIP is ~ 1 and for ZnTAPIP it is assumed to be approximately 0,8 – 0,9 based on other zinc porphyrins, such as Zn tetraphenylporphyrin [127].

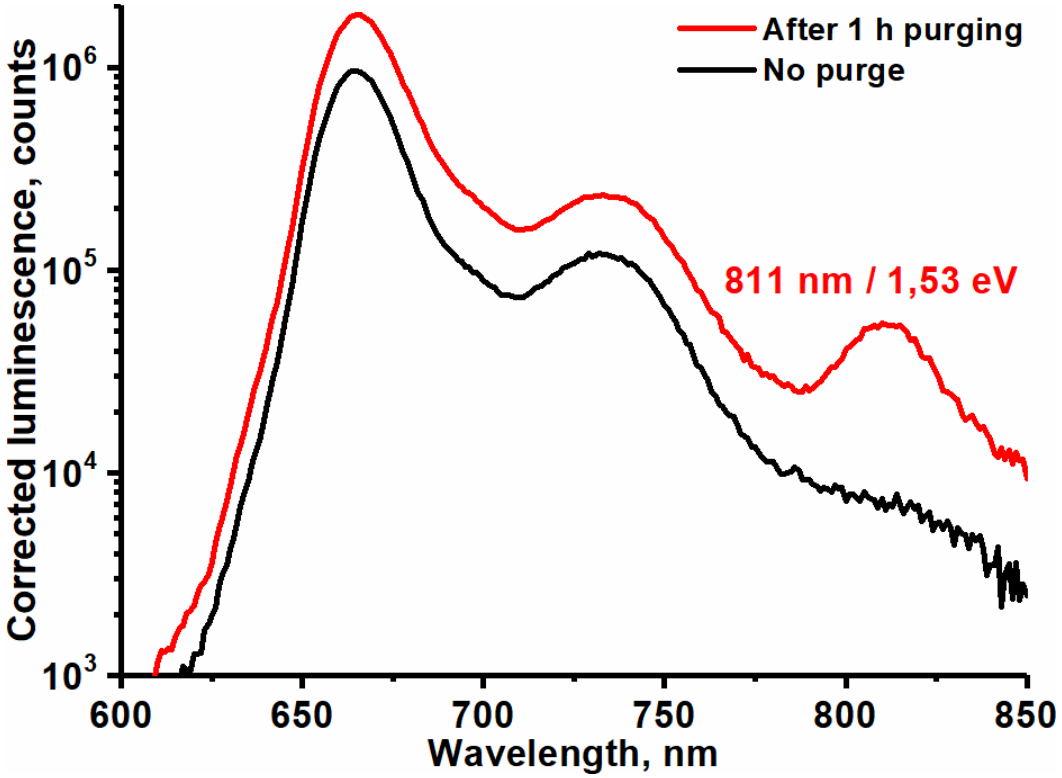

Figure 22. *The luminescence spectrum of ZnTAPIP before and after deoxygenation and excited with xenon lamp at 476 nm. NB the logarithmic vertical scale used to resolve the phosphorescence.*

The delayed fluorescence of PdTAPIP is explained by so called eosin or E-type delayed fluorescence [128] by Esipova et al. [121] E-type delayed fluorescence is typically nowadays called thermally activated delayed fluorescence (TADF) and it occurs when the singlet-triplet energy gap of a molecule is small, i.e. less than 0,1 eV or 4 k_BT, and reverse ISC can occur via thermal excitation. [129,130] Thus it is questionable that this is the mechanism behind the delayed fluorescence exhibited by PdTAPIP since the singlet-triplet energy gap is approximately 0,34 eV (the ratio of T_1 and S_1 population in thermal equilibrium would be $e^{0,34\ eV/0,0257\ eV} \approx 5{,}6 \times 10^5$). The mechanism suggested here is homo-TTA where two triplet excited PdTAPIP annihilate each other. This explanation is perhaps also applicable for the observed increase in ZnTAPIP fluorescence after deoxygenation. However, to prove that homo-TTA is indeed the mechanism behind these observations, more studies (to observe the concentration and power density dependence of the delayed fluorescence intensity) would be needed.

The fluorescence spectra of PEAP in PEG200 and DCM is shown in Figure 23. No change in fluorescence spectra between PEG200 and PEG300 was observed.

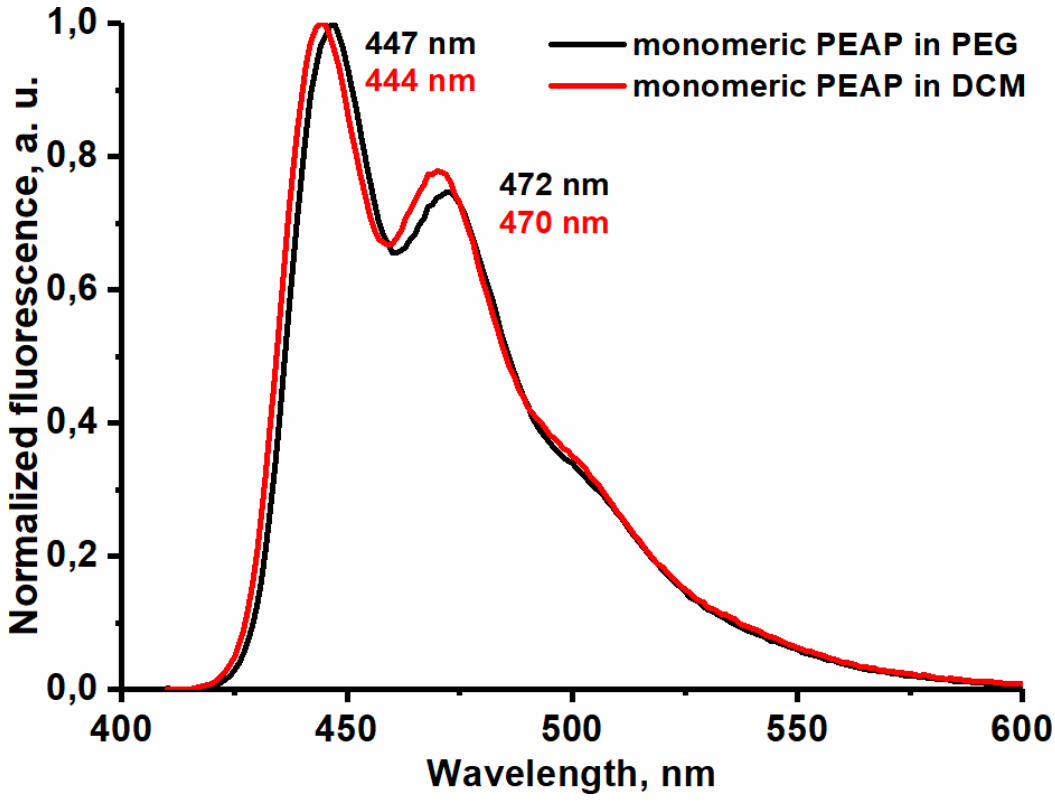

Figure 23. *Fluorescence spectra of PEAP in PEG200 and DCM. The concentration used for both measurements was 3 μM to ensure monomeric fluorescence and minimize inner filter effect. The samples were excited with a xenon lamp at 405 nm.*

5.2 Phosphorescence decays and quenching

The phosphorescence lifetimes of both porphyrin in both solvents were measured with and without PEAP as a quencher to yield the Stern-Volmer rate constants that were used with the unquenched lifetimes to calculate the triplet-triplet energy transfer rate constants. All quenching studies, titrations and power density threshold measurements were performed in both PEG200 and PEG300. PEG300 was cooled down to -5 ℃ to increase viscosity from 54 cP, provided by PEG200, to 520 cP. The phosphorescence decay curves of PdTAPIP in PEG200 in presence of PEAP as a quencher are shown in Figure 24. The phosphorescence decays of ZnTAPIP with PEAP in PEG200 are shown in Fig. 26.

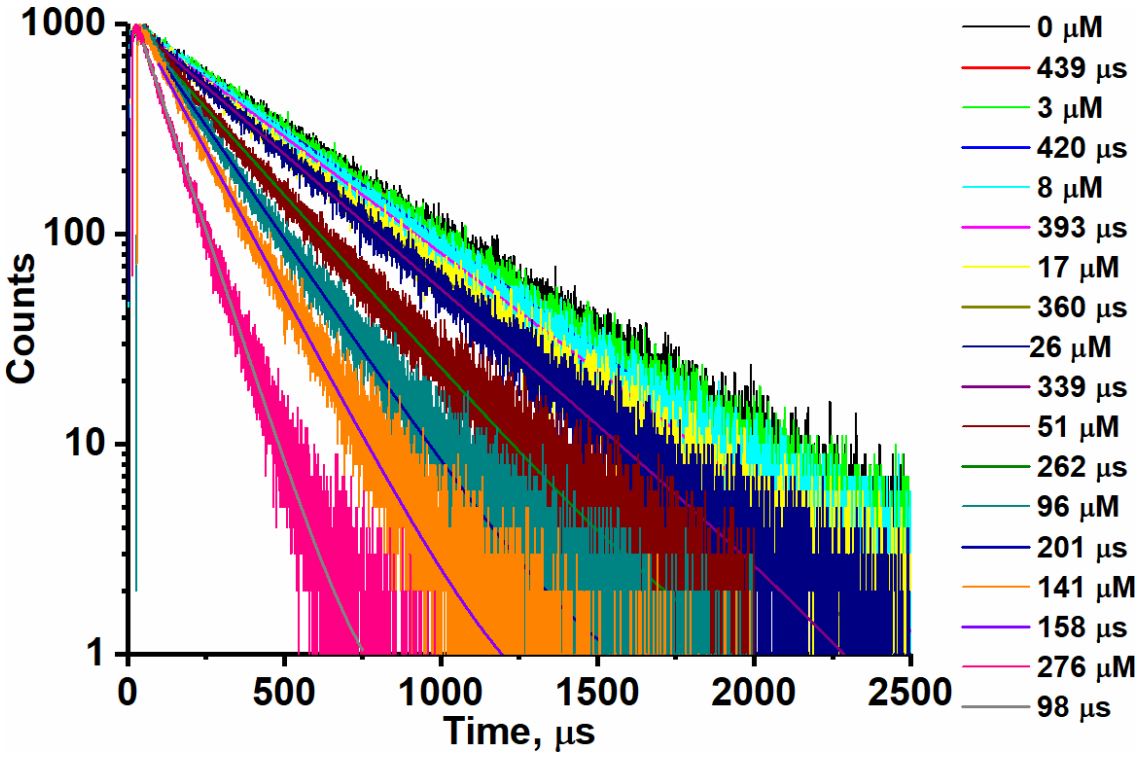

Figure 24. *Phosphorescence decays of PdTAPIP in PEG200 with increasing PEAP concentration. The time range of measurements was 4000 μs, but was cut in this figure. The legend always shows first the decay at given concentration of PEAP and then the lifetime yielded by a monoexponential fit.*

Triplet state lifetime (τ_0) of PdTAPIP in deoxygenated PEG200 is 439 μs and thus PdTAPIP can be classified as a long living sensitizer (see the list of requirements in chapter 3.3).The Stern-Volmer plot (see Eq. 14) of PdTAPIP and PEAP based on these decays is shown in Figure 25 with the value of k_{TET} calculated (see Eq. 16) based on the unquenched lifetime of PdTAPIP and the Stern-Volmer rate constant.

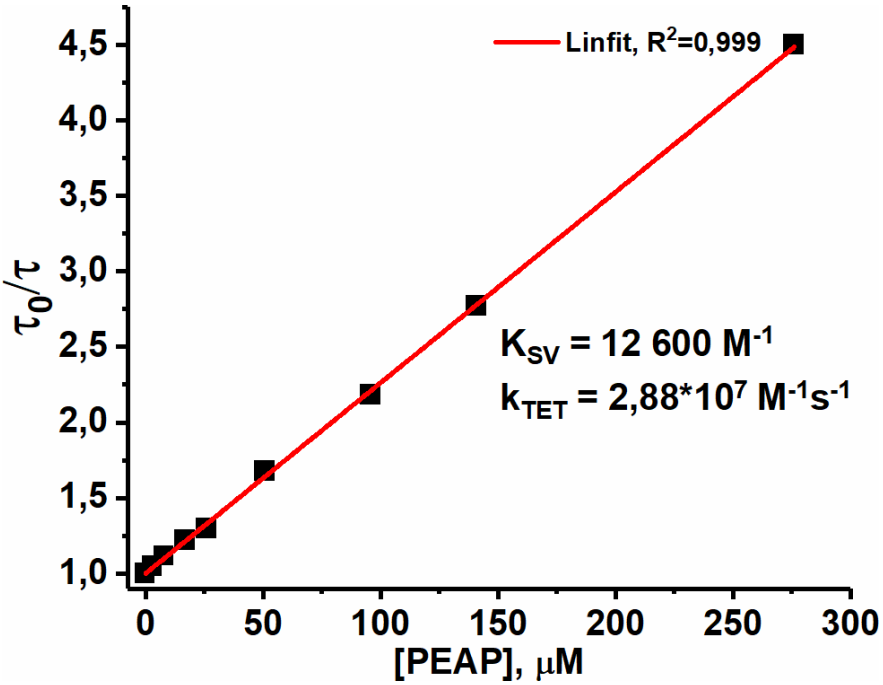

Figure 25. *The Stern-Volmer plot of PdTAPIP and PEAP in PEG200.*

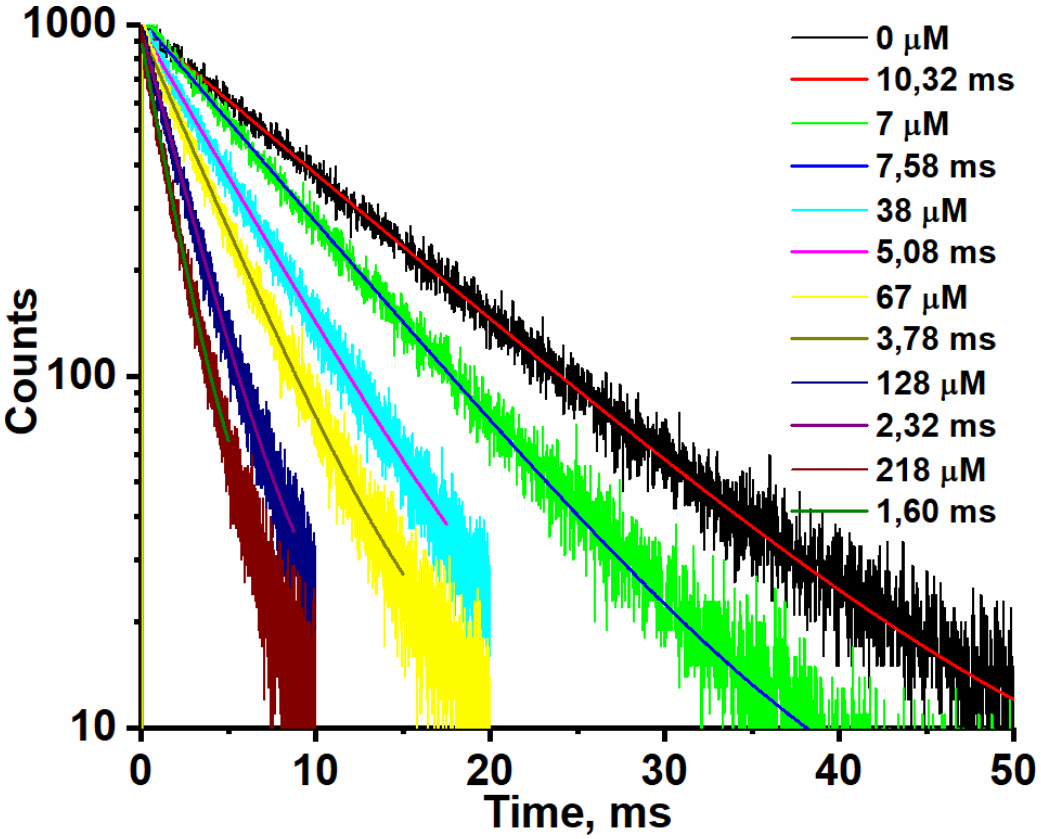

Figure 26. *Phosphorescence decays of ZnTAPIP with increasing PEAP concentration. The time ranges of the measurements were shortened as the phosphorescence was quenched by increasing lamp frequency. The fitting ranges have also been cut to reduce the effect of noise on the fit as the phosphorescence weakened.*

The small phosphorescence quantum yield of ZnTAPIP makes quenching studies somewhat challenging. Accumulation of 1000 counts at the maximum when using higher quencher concentration takes over 30 minutes indicating the weakness of the phosphorescence. This also results in smaller signal-to-noise ratio, which influences the fit to some extent and needs to be addressed when choosing the fitting ranges. The count rate is maximized by using the largest possible excitation and emission slits (13 nm by bandwidth) and using the highest possible lamp frequency. Maximizing the lamp frequency resulted in cutting the phosphorescence decays a little short.

The Stern-Volmer plot of ZnTAPIP is shown in Figure 27. τ_0 of ZnTAPIP is 10,323 ms, which means that it is an ultra-long living sensitizer. This longer lifetime explains why the Stern-Volmer rate constant of the pair ZnTAPIP/PEAP is larger than K_{SV} of PdTAPIP/PEAP. However, smaller k_{TET} results from smaller ΔE_T. Using $k_{diff} = 5 \times 10^7$ for PEG200[d] we can use Eq. 11 to get $\Delta E_T^{ZnTAPIP/PEAP}/k_B T = \ln\left(\frac{k_{diff}}{k_{TET}} - 1\right) \approx 3{,}0$ which corresponds to approx. 0,077 eV at room temperature. For PdTAPIP/PEAP the value of k_{TET} yields ΔE_T of approx. -0,01 eV. Thus, TET for ZnTAPIP is significantly endothermic and for PdTAPIP minimally exothermic. Combining these ΔE_T values and the triplet state energies of the porphyrins we can estimate the $E(T_1)$ of PEAP (in PEG200) to be 1,60–1,61 eV.

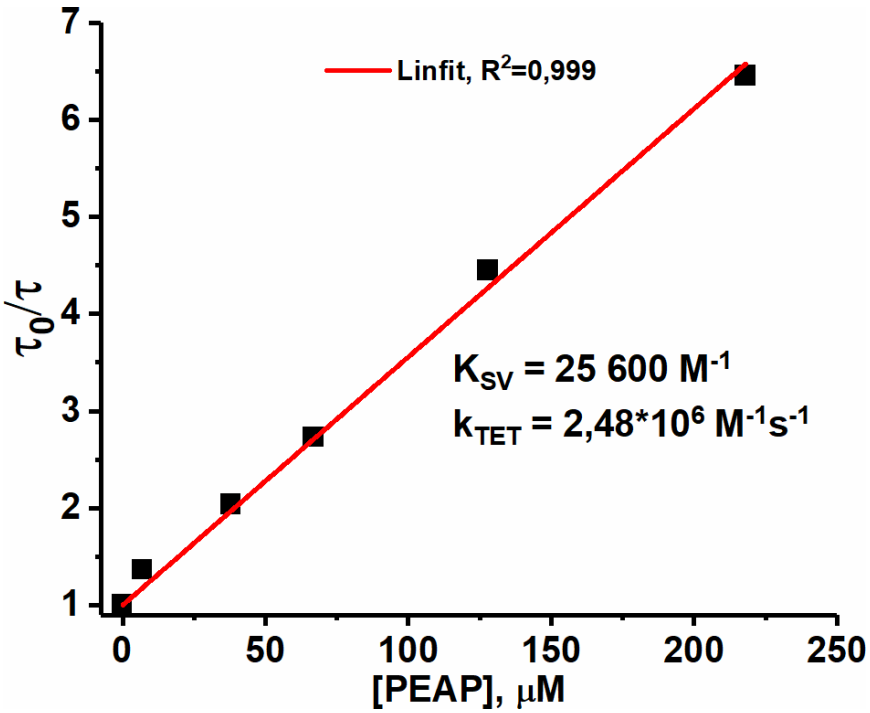

Figure 27. *The Stern-Volmer plot of ZnTAPIP and PEAP in PEG200.*

[d] This value is based on the work of Durandin et al. [107] where TET rate constants of different sensitizer/annihilator pairs in PEG200 are compared.

The same quenching studies were performed for the porphyrins in cooled down PEG300. The phosphorescence decays of PdTAPIP in -5 ℃ PEG300 are shown in Figure 28 and the corresponding SV plot is shown in Figure 29. The phosphorescence decays of ZnTAPIP and SV plot in PEG300 are shown in Figures 30 and 31, respectively.

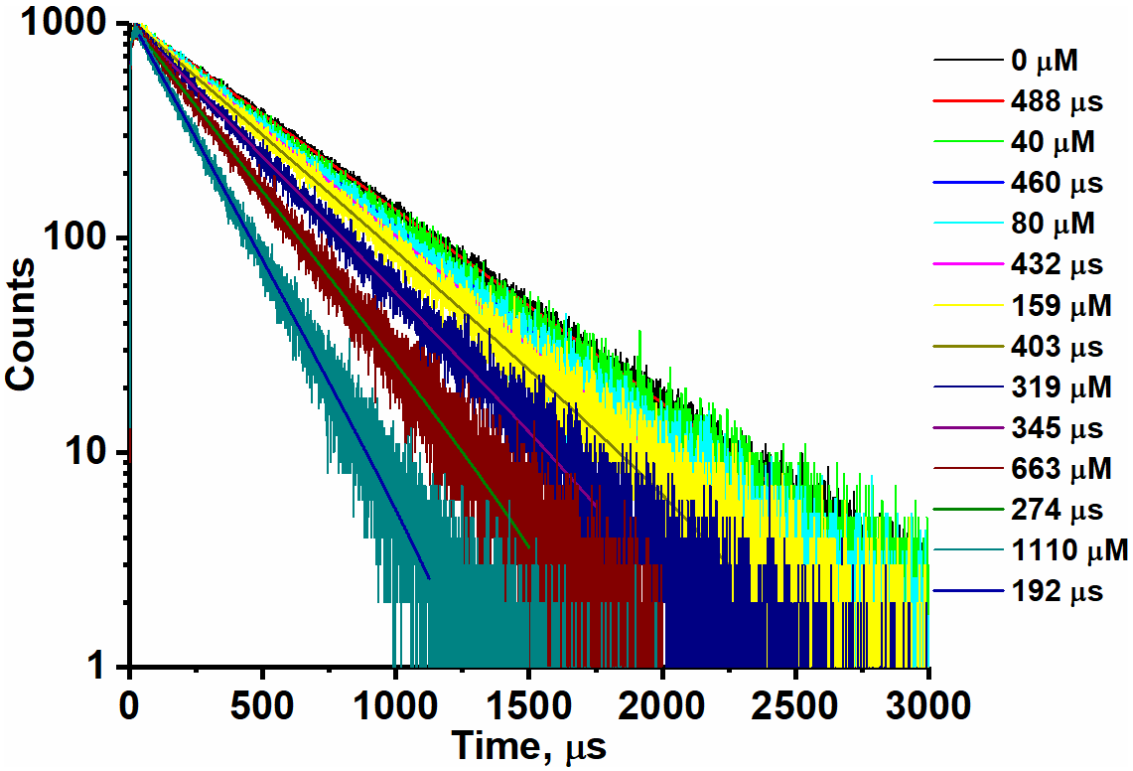

Figure 28. *Phosphorescence decays of PdTAPIP with PEAP in PEG300.*

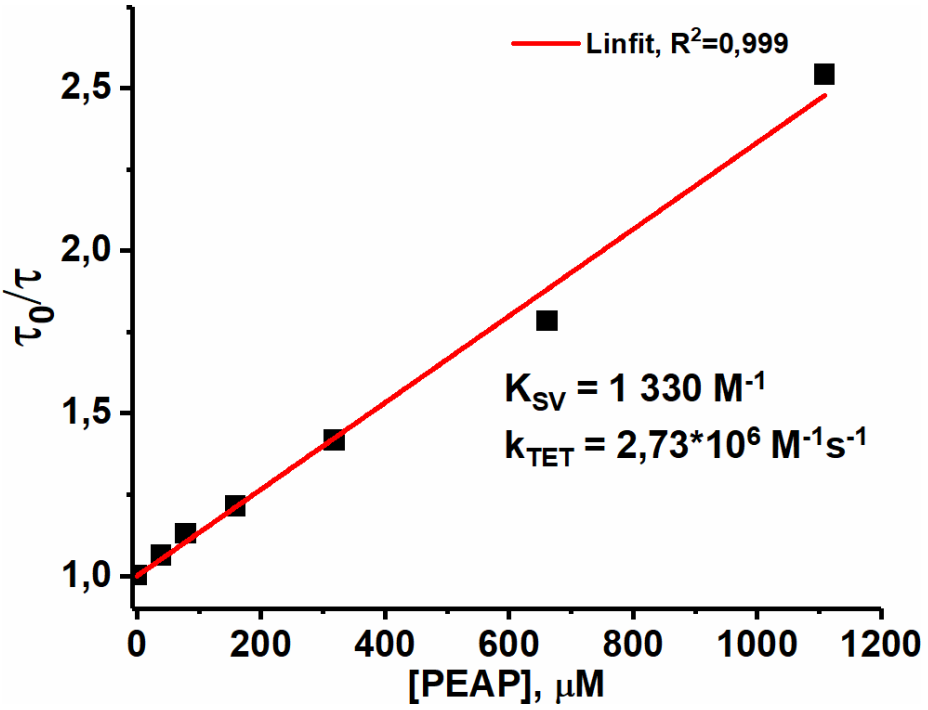

Figure 29. *Stern-Volmer plot of PdTAPIP and PEAP in PEG300.*

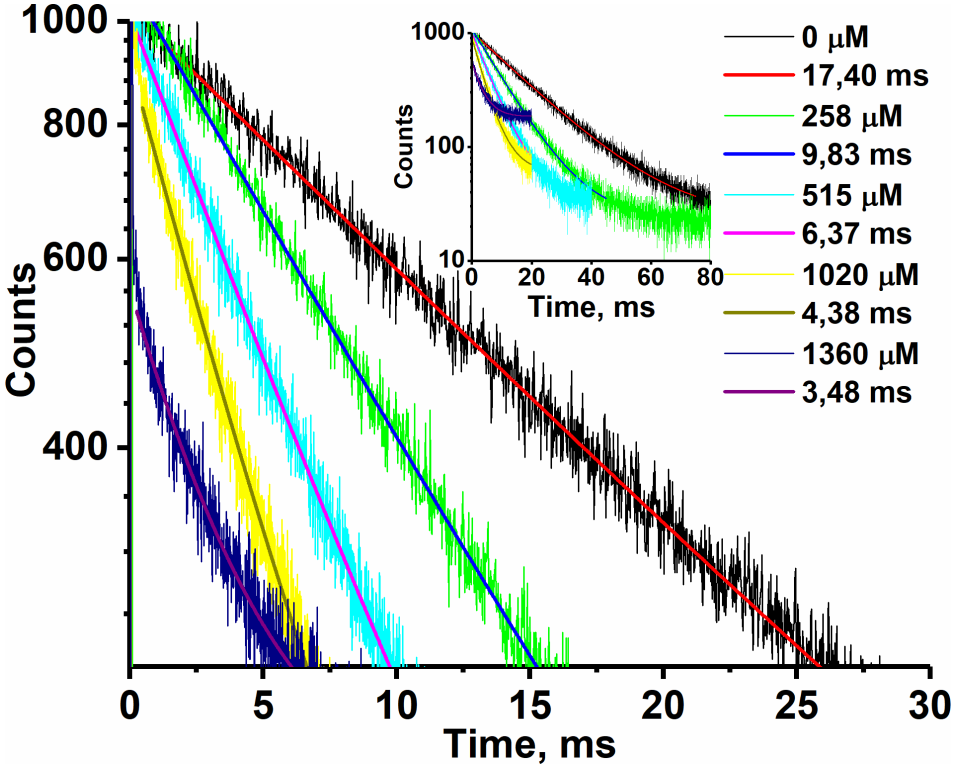

Figure 30. *Phosphorescence decays of ZnTAPIP with PEAP in PEG300. The shortest decay was cut short due to very long measurement time and high signal-to-noise ratio. Still the fit was good so it was included to the dataset. The data is "zoomed" to resolve the decays better while the inset shows the whole range.*

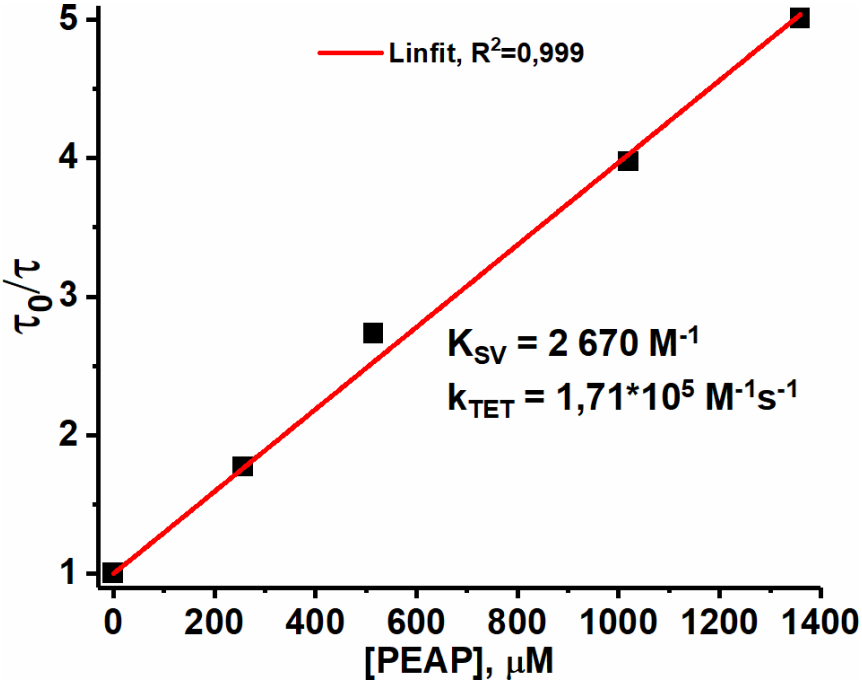

Figure 31. *Stern-Volmer plot of ZnTAPIP and PEAP in PEG300.*

In cooled PEG300 the lifetime of PdTAPIP is slightly longer than in PEG200 (488 µs vs. 439 µs). For ZnTAPIP the difference is striking: 17,40 ms vs. 10,32 ms. The longer lifetimes can be explained for both porphyrins by increased viscosity of the environment. This means that quenching by oxygen (complete removal is practically impossible), which is especially crucial in case of ZnTAPIP due to the very long lifetime, is diminished. The increased rigidity of the system may also increase the lifetimes slightly as molecular movement (e.g. rotation) is more inhibited. [131] The effect of solvent viscosity is, however, most pronounced in the rate constants as for both molecules the Stern-Volmer and TET rate constants are approximately 10 times lower. This is well in line with the viscosity values of both systems (54 cP and 520 cP for PEG200 at 20 ℃ and PEG300 at -5 ℃, respectively). Hindered diffusion and thus energy transfer means that for efficient TTAUC, higher annihilator concentration is needed. In applications where annihilator concentration is limited due to solubility or loading issues, such as polymer films or nanocarriers, a longer living sensitizer will increase energy transfer efficiency.

The energy transfer efficiency is naturally best evaluated by determining the TET efficiency (Φ_{TET}) for both molecules in both systems. Φ_{TET} was calculated with Eq. 16 at [PEAP] ranging from 10^{-6} to 3×10^{-2} M and the resulting plots are shown in Figure 32.

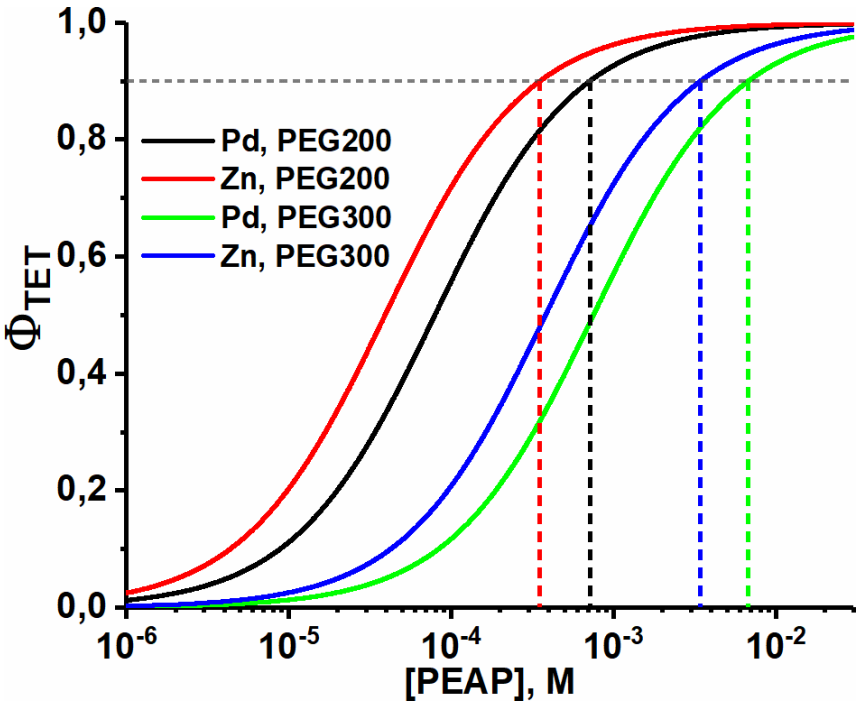

Figure 32. *The [PEAP] dependent TET efficiencies of PdTAPIP (Pd) and ZnTAPIP (Zn) in both systems. Gray dashed line represents Φ_{TET} = 90 % and the colored dashed lines the corresponding [PEAP] to achieve it.*

Figure 32 clearly shows that longer lifetime clearly favours efficient energy transfer. In order to reach 90 % TET efficiency, [PEAP] needed for PdTAPIP and ZnTAPIP in

PEG200 is 0,71 mM and 0,35 mM and in PEG300 is 6,8 mM and 3,4 mM, respectively. However, these results do not disclose the effect of reverse energy transfer, which for ZnTAPIP and PEAP is quite pronounced due to large positive ΔE_T and is addressed in the next chapter.

5.3 Annihilator titration

The effect of [PEAP] to the upconversion emission intensity was studied by titrating samples of both porphyrins in both viscous systems to find the concentration needed for maximum intensity. The optimal concentration for highest UC quantum yield basically depends on two factors: TET efficiency and consequently TTA quantum yield (see Eqs. 21 and 22) and excimer (and aggregate in some cases) formation that quenches the emission. Thus, simply, we can find an optimum concentration of PEAP for each system after which the emission intensity plateaus and starts to decrease. These titration studies are especially valuable for sensitizer/annihilator pairs exhibiting endothermic TET to also observe the suppression of reverse TET, which cannot be discerned from phosphorescence quenching. The titration curves of all porphyrins in both viscous systems are shown in Figure 33.

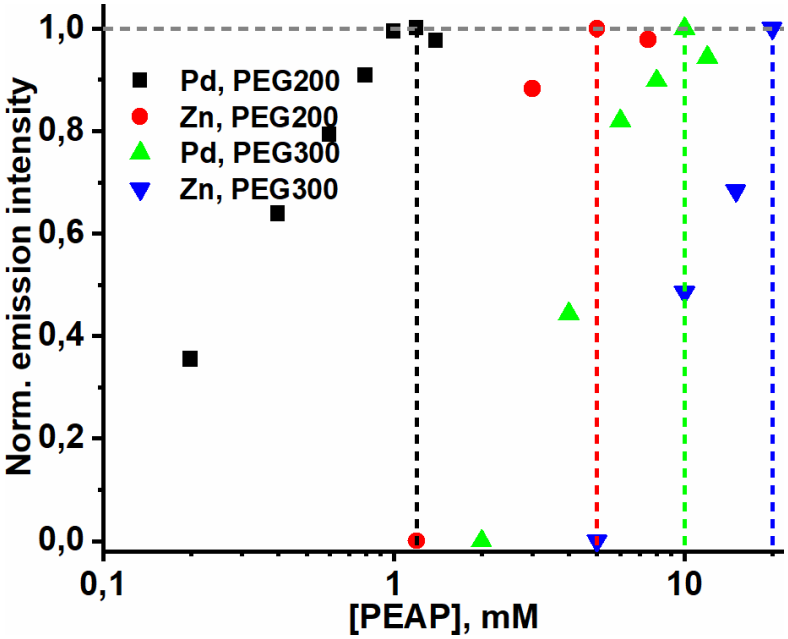

Figure 33. *Normalized upconversion emission intensity (monitored at 474 nm) of PEAP sensitized with PdTAPIP and ZnTAPIP in PEG200 and PEG300.*

Figure 33 shows that suppressing RTET requires higher [PEAP], thus maximum intensity is reached with lower [PEAP] with PdTAPIP than with ZnTAPIP. This is contrary to the TET efficiencies shown in Figure 32. It is worth mentioning that in case of ZnTAPIP in PEG300, concentration of PEAP used was limited to 20 mM (since many applications

will not allow such high concentrations and to limit consumption of materials). This 20 mM concentration is now portrayed as the concentration that yielded maximum upconversion quantum yield even though higher concentration might still be beneficial. [PEAP] that provided the highest Φ_{UC} were 1,2 mM and 10 mM for PdTAPIP and 5 and 20 mM for ZnTAPIP in PEG200 and PEG300, respectively. These concentrations were then used in power density threshold and quantum yield measurements. Naturally, lower annihilator concentrations would be needed if the solvent was less viscous, such as toluene. As a reference, Mongin et al. used 3 mM concentration of annihilator in PEG200 for their 46 µs, which gave over 90 % Φ_{TET}. [61]

5.4 Power density threshold

The power density threshold shows how low excitation intensity can be used before spontaneous decay of triplet states start to dominate over the second-order (TTA) mechanisms. Power density threshold is also the intensity that yields half of the maximum upconversion quantum yield. The upconversion emission intensity versus power density plot of PdTAPIP (absorbance at excitation wavelength 633 nm is 1,0) in PEG200 is shown in Figure 34 and the upconversion emission intensity versus power density plot of ZnTAPIP (absorbance at excitation wavelength 660 nm is 1,0) in PEG200 is shown in Figure 35.

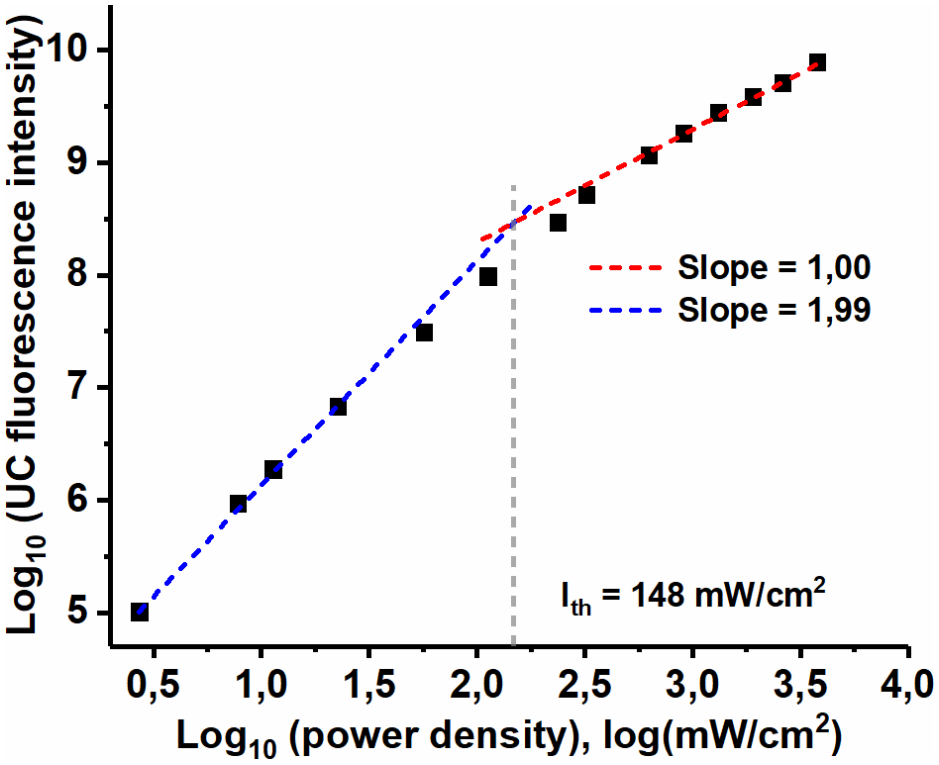

Figure 34. *Intensity of upconverted fluorescence of PEAP sensitized by PdTAPIP in PEG200 versus excitation power density in a double logarithmic plot.*

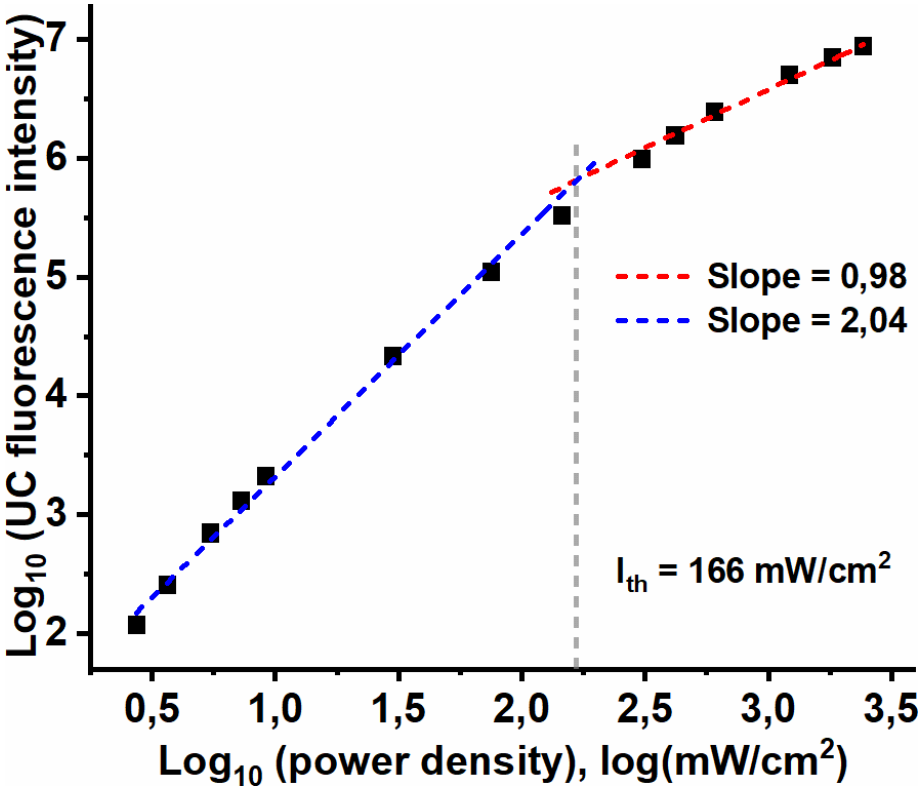

Figure 35. *Intensity of upconverted fluorescence of PEAP sensitized by ZnTAPIP in PEG200 versus excitation power density in a double logarithmic plot.*

The I_{th} values of both porphyrin in PEG200 are quite close to each other. The small difference can perhaps be explained by the smaller "total" TET efficiency between ZnTAPIP and PEAP resulting from RTET even though [PEAP] is higher than with PdTAPIP (5 mM and 1,2 mM). Both of these I_{th} values are smaller than previously reported in PEG200 by Mongin et al. (200 mW/cm^2) when using 9,10-bisphenylethynylanthracene (BPEA) as annihilator and Pt tetraphenyltetra-benzoporphyrin (PtTPTB) as sensitizer. [61] It is also remarkable, that I_{th} of ZnTAPIP sensitized TTAUC is as low in despite of quite large endothermic energy gap. The only report (found for this work) about TTAUC utilizing endothermic TET claimed no values for I_{th}, but reported that upconverted emission was still observable at 100 mW/cm$^{2.}$

The upconversion emission intensity versus power density plots of PdTAPIP (absorbance at excitation wavelength 633 nm is 2,0) and ZnTAPIP (absorbance at excitation wavelength 660 nm is 2,0) in PEG300 are shown in Figures 36 and 37, respectively.

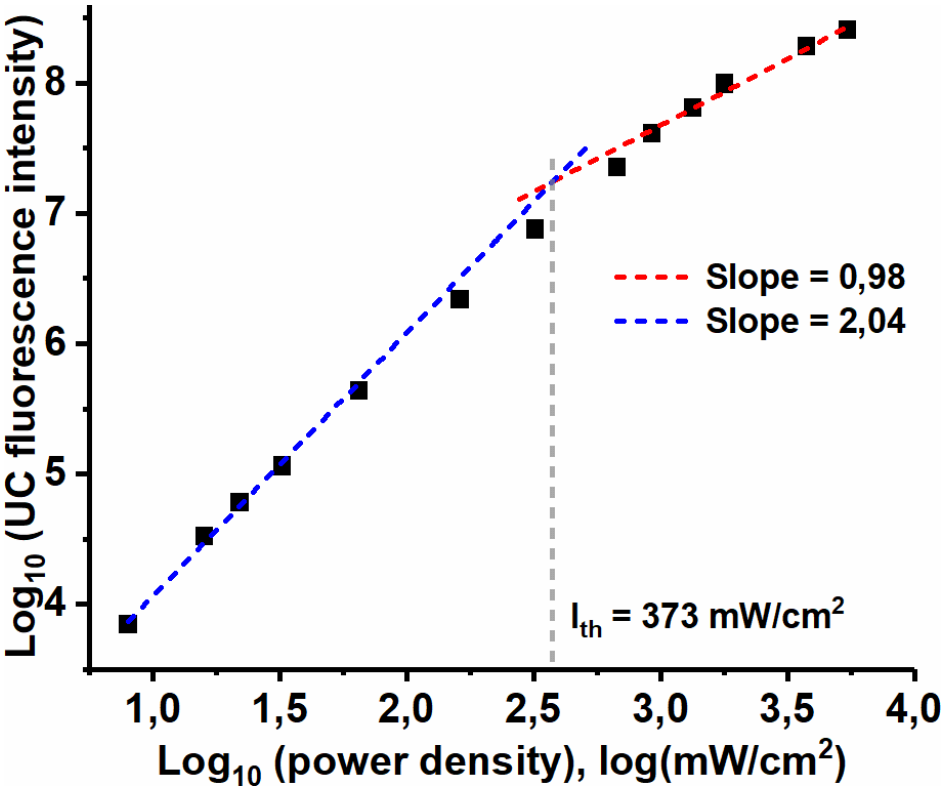

Figure 36. *Intensity of upconverted fluorescence of PEAP sensitized by PdTAPIP in PEG300 versus excitation power density in a double logarithmic plot.*

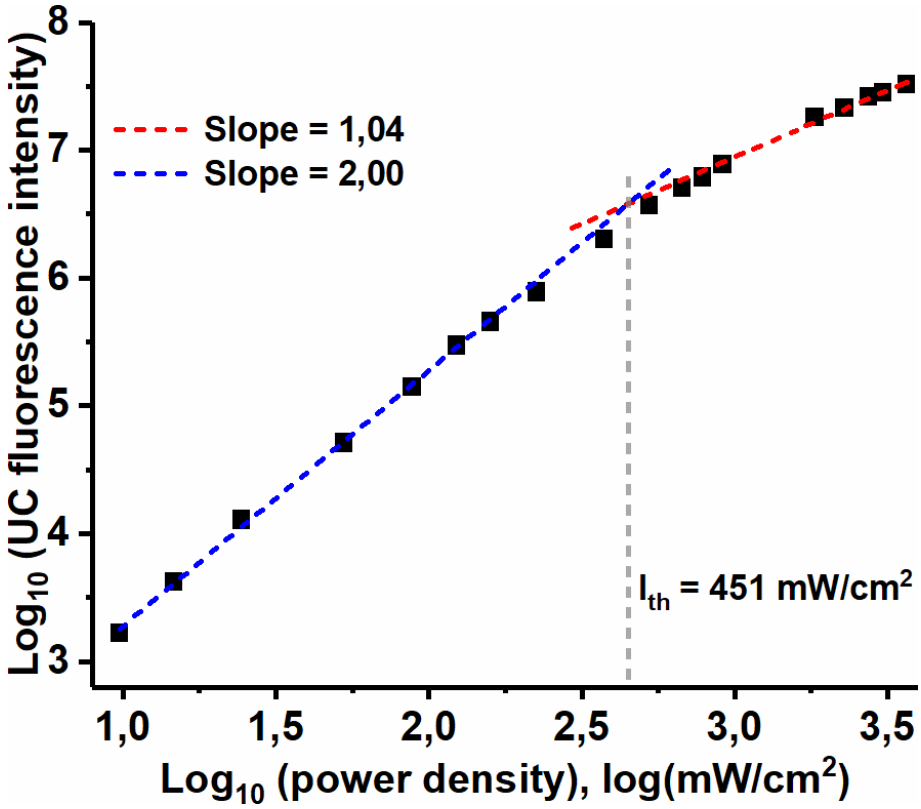

Figure 37. *Intensity of upconverted fluorescence of PEAP sensitized by ZnTAPIP in PEG300 versus excitation power density in a double logarithmic plot.*

As expected, the I_{th} values are substantially higher in more viscous PEG300 even though the sensitizer concentrations were doubled in respect to the concentrations used in PEG200 to effectively reduce I_{th} (see Eq. 25) and thus make the measurements more feasible (for example, large power densities increase photobleaching). The ratio of I_{th} between PdTAPIP and ZnTAPIP in PEG300 is approximately the same as in PEG200 (1,21 versus 1,12). The small discrepancy between these values could again possibly be explained by RTET: [PEAP] was "optimized" for ZnTAPIP in PEG200 but in PEG300 the concentration was set to 20 mM. Even higher concentration would have probably decreased I_{th}. This applies of course to every TTAUC system (but is especially advantageous in case of endothermic TET due to suppression of RTET). It is worth reminding, that while increasing annihilator concentration will decrease I_{th}, after certain level higher annihilator concentration will be detrimental for upconversion quantum yield.

5.5 Upconversion quantum yield and upconversion energy shift

The Φ_{UC} was determined by comparing the upconverted fluorescence to prompt fluorescence of a reference, in this case methylene blue and zinc phthalocyanine. Due to strong inner filter effect, the recorded spectra were corrected. The spectrum of upconverted fluorescence of PEAP sensitized by PdTAPIP in PEG200 is shown in Figure 38 and by ZnTAPIP in PEG200 in figure 39.

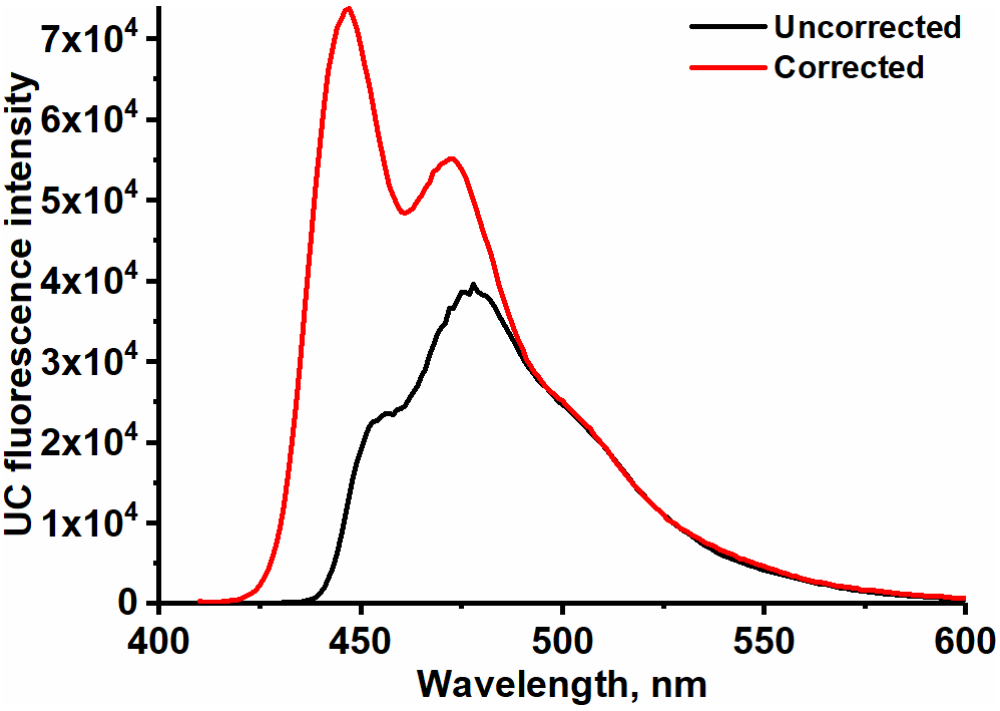

Figure 38. *Uncorrected (recorded) and corrected (with monomeric PEAP fluorescence spectrum) UC fluorescence of PEAP sensitized by PdTAPIP.*

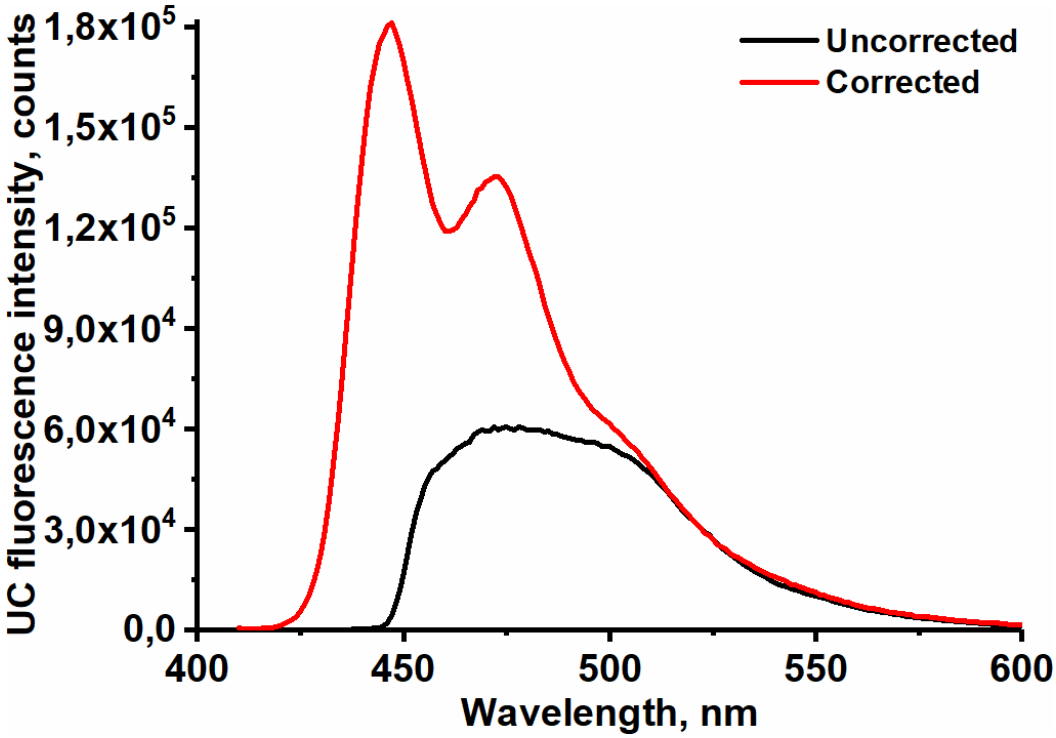

Figure 39. *Uncorrected (recorded) and corrected (with monomeric PEAP fluorescence spectrum) UC fluorescence of PEAP sensitized by ZnTAPIP.*

The power densities used (1500–2200 mW/cm^2) to obtain the maximum quantum yields of upconversion were well over the I_{th} for both porphyrins and within their linear power density dependence ranges. The recorded spectra were quite distorted by strong inner filter effect (strong absorption by PEAP and porphyrin), thus correction was needed. After correction, the integrated UC fluorescence spectra were compared with Eq. 26 to the integrated prompt fluorescence spectra of methylene blue (and also Zn phthalocyanine in case of PdTAPIP). As a result, the quantum yield of upconversion with PdTAPIP was 32,8 % and with ZnTAPIP it was 25,9 %. Φ_{UC} of ZnTAPIP was approximately 21 % smaller than Φ_{UC} of PdTAPIP which can be attributed to smaller intersystem crossing efficiency of ZnTAPIP and higher excimer formation due to higher [PEAP] utilized with ZnTAPIP (5 mM versus 1,2 mM). These quantum yields are on par with the quantum yield reported for BPEA and PtTPTB in PEG200 (Φ_{UC} = 31 %) and can be considered high. [61]

The QYs obtained in PEG200 were translated to the PEG300 system by comparing the upconversion fluorescence intensities measured for determining the power density thresholds and annihilator titration. These estimations yielded approximate Φ_{UC} of 18,6 % for PdTAPIP and 10,3 % for ZnTAPIP. The more pronounced difference between the quantum yields between the two porphyrins (45 % smaller for ZnTAPIP than PdTAPIP) is probably caused again by higher excimer formation ([PEAP] used was 20 mM and 10

mM with ZnTAPIP and PdTAPIP, respectively) and RTET in case of ZnTAPIP. For both porphyrins smaller quantum yields in PEG300 than in PEG200 were expected, since higher [PEAP] results in lower fluorescence quantum yield due to excimer formation.

For comparison of each TTAUC system, the intensities measured for determining the power density thresholds were translated into plots of quantum yield versus power density (see Figure 40). This plot could also be used to determine the power density threshold by finding the power density that yields half of the maximum quantum yield. These plots also reveal a sort of saturation point for each TTAUC system after which the Φ_{UC} does not increase with higher power density and, in fact, can even start to decrease. This saturation point occurs when the triplet population of the system approaches maximum (increased excitation intensity cannot produce any more triplet states). This approach to the maximum triplet population is also observed when the slope of upconversion intensity versus power density in a double logarithmic plot is less than 1.

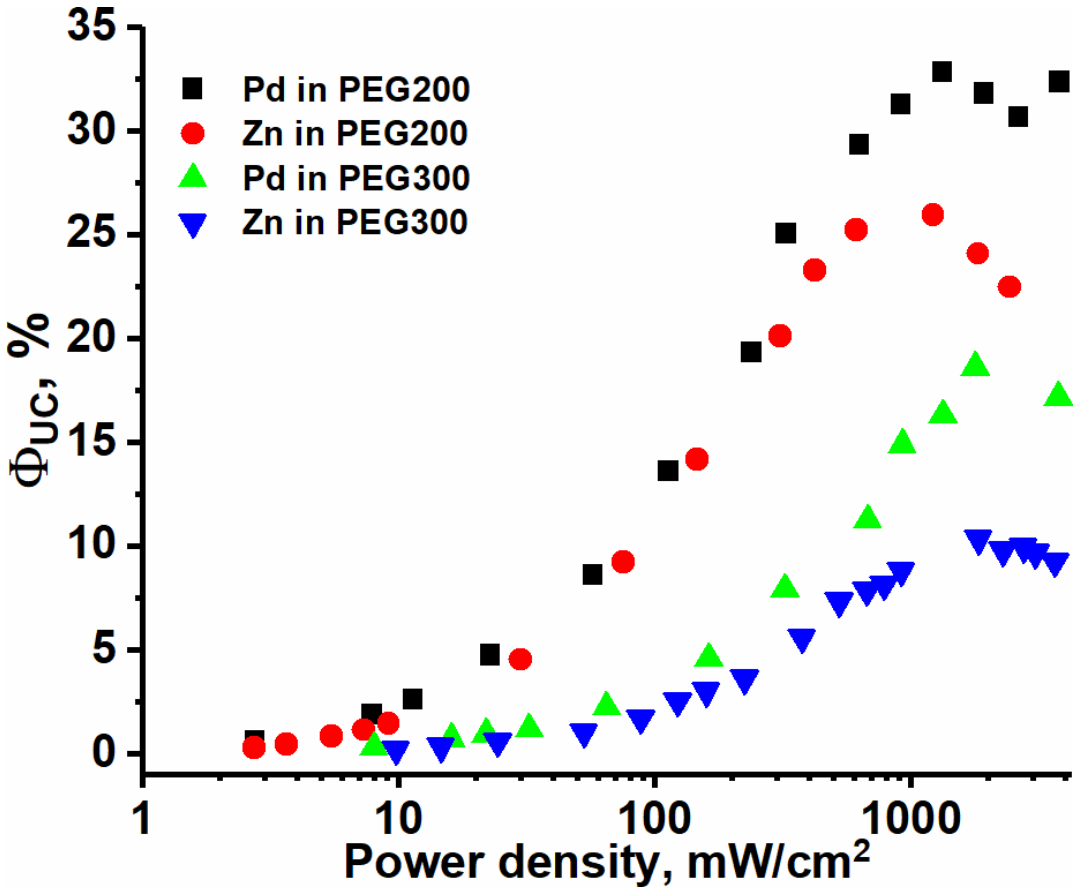

Figure 40. *Upconversion quantum yield versus power density.*

From the upconverted fluorescence spectrum of PEAP and absorption spectra of the porphyrins we can calculate the upconversion energy shifts for both systems. The energy of the blue-most (and highest intensity) peak of PEAP is 2,77 eV (448 nm) and the Q band energies of the porphyrins are 1,97 eV (PdTAPIP, 630 nm) and 1,88 eV (ZnTAPIP,

659 nm). Thus, UES for PdTAPIP/PEAP system is 0,80 eV and for ZnTAPIP/PEAP 0,89 eV. These are fairly large UES, especially when the high quantum yield is taken into account. Highest so far reported Φ_{UC} for systems exhibiting UES in the order of 0,9 eV has been 11,2 %. [93]

6. CONCLUSIONS

The objective of this work was to achieve efficient triplet-triplet annihilation upconversion in two viscous systems with porphyrins, PdTAPIP and ZnTAPIP, which have not yet been utilized as sensitizers in triplet-triplet annihilation studies and with the anthracene derivative PEAP as the annihilator. The performance of the porphyrins as sensitizers for PEAP was evaluated by determining their triplet-triplet energy transfer rate constants, power density thresholds, upconversion quantum yields and upconversion energy shifts. In addition to upconversion studies, the basic photophysical properties, absorption, luminescence and triplet state lifetimes, of the porphyrins were characterized. These results are compiled in Table 2.

Table 2. *The essential results of the thesis. τ_0 is the unquenched triplet state lifetime of the porphyrin, k_{TET} is the triplet-triplet energy transfer rate constant from porphyrin to PEAP, ΔE_T is the triplet energy gap between porphyrin and PEAP. [S] is the porphyrin (sensitizer) concentration required for absorbance of 1 or 2 at the excitation wavelength and [PEAP] is the concentration that yields highest upconversion quantum yield and used for upconversion studies. I_{th} is the power density threshold of each upconversion system, Φ_{UC} is the maximum upconversion quantum yield of each system and UES is the upconversion energy shift, i.e. the difference between PEAP emission and porphyrin absorption energy.*

Sensitizer	**PdTAPIP**		**ZnTAPIP**	
Viscosity, cP	54	520	54	520
τ_0, µs	438	488	10 300	17 400
k_{TET}, $M^{-1}s^{-1}$	$2{,}9*10^7$	$2{,}7*10^6$	$2{,}5*10^6$	$1{,}7*10^5$
ΔE_T, k_BT / eV	-0,4 / -0,01		3 / 0,077	
[S], µM	4	8	5	10
[PEAP], mM	1,2	10	5	20
I_{th}, mW/cm^2	148	373	166	451
Φ_{UC}, %	33	19	26	10
UES, eV	0,80		0,89	

It can be concluded, the objectives set for the thesis were achieved: both porphyrin is a potent sensitizer for efficient TTAUC, thanks to their high molar absorption coefficients and long triplet state lifetimes. The efficiency is manifested by low power thresholds, high quantum yields of upconversion while exhibiting large upconversion energy shifts. These results proof that both ZnTAPIP and PdTAPIP can be utilized as sensitizers in viscous TTAUC systems. Especially PdTAPIP seems desirable sensitizer for PEAP since lower amounts of PEAP are required to yield efficient TTAUC. Altogether, both sensitizer and the TTAUC systems they were utilized for are state of the art. The next step paved by this work would be utilizing these porphyrins for TTAUC in solid-state devices or nanocarriers and in real applications, such as micellar drug delivery systems.

REFERENCES

[1] J. Zhou, Q. Liu, W. Feng, Y. Sun and F. Li. "Upconversion Luminescent Materials: Advances and Applications". *Chemical Reviews*. vol. 115, no. 1, pp. 395–465, 2015.

[2] C.A. Parker and C.G. Hatchard. "Delayed fluorescence from solutions of anthracene and phenanthrene". *Proceedings of the Royal Society of London Series A Mathematical and Physical Sciences*. vol. 269, no. 1339, pp. 574–84, 1962.

[3] T.N. Singh-Rachford and F.N. Castellano. "Photon upconversion based on sensitized triplet-triplet annihilation". *Coordination Chemistry Reviews*. vol. 254, no. 21–22, pp. 2560–73, 2010.

[4] M. Göppert-Mayer. "Über Elementarakte mit zwei Quantensprüngen". *Annalen der Physik*. vol. 401, no. 3, pp. 273–94, 1931.

[5] W. Kaiser and C.G.B. Garrett. "Two-Photon Excitation in CaF2: Eu2+". *Phys Rev Lett*. vol. 7, no. 6, pp. 229–31, 1961.

[6] P.A. Franken, A.E. Hill, C.W. Peters and G. Weinreich. "Generation of Optical Harmonics". *Phys Rev Lett*. vol. 7, no. 4, pp. 118–9, 1961.

[7] N. Bloembergen and P.S. Pershan. "Light Waves at the Boundary of Nonlinear Media". *Phys Rev*. vol. 128, no. 2, pp. 606–22, 1962.

[8] F. Auzel. "Upconversion and Anti-Stokes Processes with f and d Ions in Solids". *Chemical Reviews*. vol. 104, no. 1, pp. 139–74, 2004.

[9] F. Auzel. "Compteur quantique par transfert denergie de Yb3+ a Tm3+ dans un tungstate mixte et dans un verre germanate". *Comptes Rendus Hebdomadaires Des Seances De L Academie Des Sciences Serie B*. vol. 263, no. 14, pp. 819, 1966.

[10] D.H. Weingarten, M.D. LaCount, J. van de Lagemaat, G. Rumbles, M.T. Lusk and S.E. Shaheen. "Experimental demonstration of photon upconversion via cooperative energy pooling". *Nature Communications*. vol. 8, pp. 14808, 2017.

[11] C.A. Parker and C.G. Hatchard. "Sensitised anti-stokes delayed fluorescence". *Proceedings of the Chemical Society*. pp. 386–7, 1962.

[12] Y.C. Simon and C. Weder. "Low-power photon upconversion through triplet–triplet annihilation in polymers". *J Mater Chem*. vol. 22, no. 39, pp. 20817–30, 2012.

[13] P. Ceroni. "Energy Up-Conversion by Low-Power Excitation: New Applications of an Old Concept". *Chemistry – A European Journal*. vol. 17, no. 35, pp. 9560–4, 2011.

[14] J. Zhao, S. Ji, W. Wu, W. Wu, H. Guo, J. Sun, et al. "Transition metal complexes with strong absorption of visible light and long-lived triplet excited states: from molecular design to applications". *RSC Adv*. vol. 2, no. 5, pp. 1712–28, 2012.

[15] T.F. Schulze and T.W. Schmidt. "Photochemical upconversion: present status and prospects for its application to solar energy conversion". *Energy Environ Sci*. vol. 8, no. 1, pp. 103–25, 2015.

[16] J. Zhao, S. Ji and H. Guo. "Triplet–triplet annihilation based upconversion: from triplet sensitizers and triplet acceptors to upconversion quantum yields". *RSC Adv*. vol. 1, no. 6, pp. 937–50, 2011.

[17] X. Zhu, Q. Su, W. Feng and F. Li. "Anti-Stokes shift luminescent materials for bio-applications". *Chem Soc Rev*. vol. 46, no. 4, pp. 1025–39, 2017.

[18] V. Gray, D. Dzebo, M. Abrahamsson, B. Albinsson and K. Moth-Poulsen. "Triplet–triplet annihilation photon-upconversion: towards solar energy applications". *Phys Chem Chem Phys*. vol. 16, no. 22, pp. 10345–52, 2014.

[19] A. Nattestad, Y.Y. Cheng, R.W. MacQueen, T.F. Schulze, F.W. Thompson, A.J. Mozer, et al. "Dye-Sensitized Solar Cell with Integrated Triplet–Triplet Annihilation

Upconversion System". *The Journal of Physical Chemistry Letters*. vol. 4, no. 12, pp. 2073–8, 2013.

[20] Y.Y. Cheng, A. Nattestad, T.F. Schulze, R.W. MacQueen, B. Fückel, K. Lips, et al. "Increased upconversion performance for thin film solar cells: a trimolecular composition". *Chem Sci*. vol. 7, no. 1, pp. 559–68, 2016.

[21] S. Baluschev, V. Yakutkin, G. Wegner, T. Miteva, G. Nelles, A. Yasuda, et al. "Upconversion with ultrabroad excitation band: Simultaneous use of two sensitizers". *Applied Physics Letters*. vol. 90, no. 18, pp. 181103, 2007.

[22] J.-H. Kim and J.-H. Kim. "Encapsulated Triplet–Triplet Annihilation-Based Upconversion in the Aqueous Phase for Sub-Band-Gap Semiconductor Photocatalysis". *Journal of the American Chemical Society*. vol. 134, no. 42, pp. 17478–81, 2012.

[23] N.J. Ekins-Daukes and T.W. Schmidt. "A molecular approach to the intermediate band solar cell: The symmetric case". *Applied Physics Letters*. vol. 93, no. 6, pp. 63507, 2008.

[24] T. Trupke, A. Shalav, B.S. Richards, P. Würfel and M.A. Green. "Efficiency enhancement of solar cells by luminescent up-conversion of sunlight". *Solar Energy Materials and Solar Cells*. vol. 90, no. 18, pp. 3327–38, 2006.

[25] R.R. Islangulov and F.N. Castellano. "Photochemical Upconversion: Anthracene Dimerization Sensitized to Visible Light by a RuII Chromophore". *Angewandte Chemie International Edition*. vol. 45, no. 36, pp. 5957–9, 2006.

[26] K. Börjesson, D. Dzebo, B. Albinsson and K. Moth-Poulsen. "Photon upconversion facilitated molecular solar energy storage". *J Mater Chem A*. vol. 1, no. 30, pp. 8521–4, 2013.

[27] Z. Jiang, M. Xu, F. Li and Y. Yu. "Red-Light-Controllable Liquid-Crystal Soft Actuators via Low-Power Excited Upconversion Based on Triplet–Triplet Annihilation". *Journal of the American Chemical Society*. vol. 135, no. 44, pp. 16446–53, 2013.

[28] C. Murawski, K. Leo and M.C. Gather. "Efficiency Roll-Off in Organic Light-Emitting Diodes". *Advanced Materials*. vol. 25, no. 47, pp. 6801–27, 2013.

[29] D.Y. Kondakov. "Triplet-triplet annihilation in highly efficient fluorescent organic light-emitting diodes: current state and future outlook". *Philosophical Transactions of the Royal Society A: Mathematical, Physical and Engineering Sciences*. vol. 373, no. 2044, pp. 20140321, 2015.

[30] M.B. Smith and J. Michl. "Singlet Fission". *Chemical Reviews*. vol. 110, no. 11, pp. 6891–936, 2010.

[31] C. Wohnhaas, V. Mailänder, M. Dröge, M.A. Filatov, D. Busko, Y. Avlasevich, et al. "Triplet–Triplet Annihilation Upconversion Based Nanocapsules for Bioimaging Under Excitation by Red and Deep-Red Light". *Macromolecular Bioscience*. vol. 13, no. 10, pp. 1422–30, 2013.

[32] O.S. Kwon, H.S. Song, J. Conde, H. Kim, N. Artzi and J.-H. Kim. "Dual-Color Emissive Upconversion Nanocapsules for Differential Cancer Bioimaging In Vivo". *ACS Nano*. vol. 10, no. 1, pp. 1512–21, 2016.

[33] Q. Liu, B. Yin, T. Yang, Y. Yang, Z. Shen, P. Yao, et al. "A General Strategy for Biocompatible, High-Effective Upconversion Nanocapsules Based on Triplet–Triplet Annihilation". *Journal of the American Chemical Society*. vol. 135, no. 13, pp. 5029–37, 2013.

[34] B.P. Timko, T. Dvir and D.S. Kohane. "Remotely Triggerable Drug Delivery Systems". *Advanced Materials*. vol. 22, no. 44, pp. 4925–43, 2010.

[35] S.H.C. Askes, A. Bahreman and S. Bonnet. "Activation of a Photodissociative Ruthenium Complex by Triplet-Triplet Annihilation Upconversion in Liposomes". *Angewandte Chemie International Edition*. vol. 53, no. 4, pp. 1029–33, 2014.

[36] S.H.C. Askes, M. Kloz, G. Bruylants, J.T.M. Kennis and S. Bonnet. "Triplet–triplet annihilation upconversion followed by FRET for the red light activation of a photodissociative ruthenium complex in liposomes". *Physical Chemistry Chemical*

Physics. vol. 17, no. 41, pp. 27380–90, 2015.
[37] W. Wang, Q. Liu, C. Zhan, A. Barhoumi, T. Yang, R.G. Wylie, et al. "Efficient Triplet–Triplet Annihilation-Based Upconversion for Nanoparticle Phototargeting". *Nano Letters*. vol. 15, no. 10, pp. 6332–8, 2015.
[38] Q. Liu, W. Wang, C. Zhan, T. Yang and D.S. Kohane. "Enhanced Precision of Nanoparticle Phototargeting in Vivo at a Safe Irradiance". *Nano Letters*. vol. 16, no. 7, pp. 4516–20, 2016.
[39] T.J. Penfold, E. Gindensperger, C. Daniel and C.M. Marian. "Spin-Vibronic Mechanism for Intersystem Crossing". *Chemical Reviews*. vol. 118, no. 15, pp. 6975–7025, 2018.
[40] P.A.M. Dirac and H.R. Fowler. "The quantum theory of the electron". *Proceedings of the Royal Society of London Series A, Containing Papers of a Mathematical and Physical Character*. vol. 117, no. 778, pp. 610–24, 1928.
[41] G. Baryshnikov, B. Minaev and H. Ågren. "Theory and Calculation of the Phosphorescence Phenomenon". *Chemical Reviews*. vol. 117, no. 9, pp. 6500–37, 2017.
[42] W. Pauli. "Zur Quantenmechanik des magnetischen Elektrons". *Zeitschrift für Physik*. vol. 43, no. 9–10, pp. 601–23, 1927.
[43] S. Koseki, M.W. Schmidt and M.S. Gordon. "MCSCF/6-31G(d,p) calculations of one-electron spin-orbit coupling constants in diatomic molecules". *The Journal of Physical Chemistry*. vol. 96, no. 26, pp. 10768–72, 1992.
[44] D.S. McClure. "Triplet-Singlet Transitions in Organic Molecules. Lifetime Measurements of the Triplet State". *The Journal of Chemical Physics*. vol. 17, no. 10, pp. 905–13, 1949.
[45] M. Born and R. Oppenheimer. "Zur Quantentheorie der Molekeln". *Annalen der Physik*. vol. 389, no. 20, pp. 457–84, 1927.
[46] G.A. Worth and L.S. Cederbaum. "BEYOND BORN-OPPENHEIMER: Molecular Dynamics Through a Conical Intersection". *Annual Review of Physical Chemistry*. vol. 55, no. 1, pp. 127–58, 2004.
[47] A.C. Albrecht. "Vibronic—Spin-Orbit Perturbations and the Assignment of the Lowest Triplet State of Benzene". *The Journal of Chemical Physics*. vol. 38, no. 2, pp. 354–65, 1963.
[48] P.A.M. Dirac. "The Quantum Theory of the Emission and Absorption of Radiation". *Proceedings of the Royal Society A: Mathematical, Physical and Engineering Sciences*. vol. 114, no. 767, pp. 243–65, 1927.
[49] M.A. El-Sayed. "Spin—Orbit Coupling and the Radiationless Processes in Nitrogen Heterocyclics". *The Journal of Chemical Physics*. vol. 38, no. 12, pp. 2834–8, 1963.
[50] S. Perun, J. Tatchen and C.M. Marian. "Singlet and Triplet Excited States and Intersystem Crossing in Free-Base Porphyrin: TDDFT and DFT/MRCI Study". *ChemPhysChem*. vol. 9, no. 2, pp. 282–92, 2008.
[51] V. Balzani, A. Juris, M. Venturi, S. Campagna and S. Serroni. "Luminescent and Redox-Active Polynuclear Transition Metal Complexes". *Chemical Reviews*. vol. 96, no. 2, pp. 759–834, 1996.
[52] R. Englman and J. Jortner. "The energy gap law for radiationless transitions in large molecules". *Molecular Physics*. vol. 18, no. 2, pp. 145–64, 1970.
[53] A. Terenin and V. Ermolaev. "Sensitized phosphorescence in organic solutions at low temperature. Energy transfer between triplet states". *Transactions of the Faraday Society*. vol. 52, pp. 1042, 1956.
[54] F. Zapata, M. Marazzi, O. Castaño, A.U. Acuña and L.M. Frutos. "Definition and determination of the triplet-triplet energy transfer reaction coordinate". *The Journal of Chemical Physics*. vol. 140, no. 3, pp. 034102, 2014.
[55] D.L. Dexter. "A Theory of Sensitized Luminescence in Solids". *The Journal of Chemical Physics*. vol. 21, no. 5, pp. 836–50, 1953.
[56] C. Serpa, L.G. Arnaut, S.J. Formosinho and K.R. Naqvi. "Calculation of triplet–

triplet energy transfer rates from emission and absorption spectra. The quenching of hemicarcerated triplet biacetyl by aromatic hydrocarbons". *Photochem Photobiol Sci*. vol. 2, no. 5, pp. 616–23, 2003.

[57] A. Monguzzi, R. Tubino and F. Meinardi. "Upconversion-induced delayed fluorescence in multicomponent organic systems: Role of Dexter energy transfer". *Physical Review B*. vol. 77, no. 15, pp. 155122–4, 2008.

[58] M. Inokuti and F. Hirayama. "Influence of Energy Transfer by the Exchange Mechanism on Donor Luminescence". *The Journal of Chemical Physics*. vol. 43, no. 6, pp. 1978–89, 1965.

[59] T. Förster. "Zwischenmolekulare Energiewanderung und Fluoreszenz". *Annalen der Physik*. vol. 437, no. 1-2, pp. 55–75, 1948.

[60] J. Saltiel, P.T. Shannon, O.C. Zafiriou and A.K. Uriarte. "A case of fully diffusion-controlled exothermic triplet excitation transfer". *Journal of the American Chemical Society*. vol. 102, no. 22, pp. 6799–808, 1980.

[61] C. Mongin, J.H. Golden and F.N. Castellano. "Liquid PEG Polymers Containing Antioxidants: A Versatile Platform for Studying Oxygen-Sensitive Photochemical Processes". *ACS Applied Materials & Interfaces*. vol. 8, no. 36, pp. 24038–48, 2016.

[62] A. Einstein. "Über die von der molekularkinetischen Theorie der Wärme geforderte Bewegung von in ruhenden Flüssigkeiten suspendierten Teilchen". *Annalen der Physik*. vol. 322, no. 8, pp. 549–60, 1905.

[63] G. Porter and F. Wilkinson. "Energy transfer from the triplet state". *Proceedings of the Royal Society of London Series A Mathematical and Physical Sciences*. vol. 264, no. 1316, pp. 1–18, 1961.

[64] K. Sandros and H.L.J. Bäckström. "II. Further Studies of the Quenching of Biacetyl Phosphorescence in Solution". *Acta Chimica Scandinavica*. vol. 16, pp. 958–68, 1962.

[65] S. Arrhenius. "Über die Dissociationswärme und den Einfluss der Temperatur auf den Dissociationsgrad der Elektrolyte". *Zeitschrift für Physikalische Chemie*. vol. 4U, no. 1, pp. 96–116, 1889.

[66] K. Sandros. "Transfer of Triplet State Energy in Fluid Solutions. III. Reversible Energy Transfer.". *Acta Chimica Scandinavica*. vol. 18, pp. 2355–74, 1964.

[67] Y.Y. Cheng, B. Fückel, T. Khoury, R.G.C.R. Clady, N.J. Ekins-Daukes, M.J. Crossley, et al. "Entropically Driven Photochemical Upconversion". *The Journal of Physical Chemistry A*. vol. 115, no. 6, pp. 1047–53, 2011.

[68] O. Stern and M. Volmer. "Über die Abklingzeit der Fluoreszenz". *Physik Zeitschr*. vol. 20, pp. 183–8, 1919.

[69] C. Bohne, E.B. Abuin and J.C. Scaiano. "Characterization of the triplet-triplet annihilation process of pyrene and several derivatives under laser excitation". *Journal of the American Chemical Society*. vol. 112, no. 11, pp. 4226–31, 1990.

[70] W. Zhao and F.N. Castellano. "Upconverted Emission from Pyrene and Di-tert-butylpyrene Using Ir(ppy)3 as Triplet Sensitizer". *The Journal of Physical Chemistry A*. vol. 110, no. 40, pp. 11440–5, 2006.

[71] S.H.C. Askes, P. Brodie, G. Bruylants and S. Bonnet. "Temperature Dependence of Triplet–Triplet Annihilation Upconversion in Phospholipid Membranes". *The Journal of Physical Chemistry B*. vol. 121, no. 4, pp. 780–6, 2017.

[72] S.H.C. Askes, V.C. Leeuwenburgh, W. Pomp, H. Arjmandi-Tash, S. Tanase, T. Schmidt, et al. "Water-Dispersible Silica-Coated Upconverting Liposomes: Can a Thin Silica Layer Protect TTA-UC against Oxygen Quenching?". *ACS Biomaterials Science & Engineering*. vol. 3, no. 3, pp. 322–34, 2017.

[73] S.H.C. Askes, W. Pomp, S.L. Hopkins, A. Kros, S. Wu, T. Schmidt, et al. "Imaging Upconverting Polymersomes in Cancer Cells: Biocompatible Antioxidants Brighten Triplet-Triplet Annihilation Upconversion". *Small*. vol. 12, no. 40, pp. 5579–90, 2016.

[74] Q. Liu, W. Feng, T. Yang, T. Yi and F. Li. "Upconversion luminescence imaging

of cells and small animals". *Nature Protocols*. vol. 8, no. 10, pp. 2033–44, 2013.
[75] C.A. Parker and T.A. Joyce. "Delayed fluorescence of anthracene and some substituted anthracenes". *Chemical Communications (London)*. no. 15, pp. 744–5, 1967.
[76] C.A. Parker and E.J. Bowen. "Sensitized *P*-type delayed fluorescence". *Proceedings of the Royal Society of London Series A Mathematical and Physical Sciences*. vol. 276, no. 1364, pp. 125–35, 1963.
[77] A. Monguzzi, R. Tubino, S. Hoseinkhani, M. Campione and F. Meinardi. "Low power, non-coherent sensitized photon up-conversion: modelling and perspectives". *Phys Chem Chem Phys*. vol. 14, no. 13, pp. 4322–32, 2012.
[78] A.J. McLean and T.G. Truscott. "Faraday communications. Efficiency of triplet-photosensitised singlet oxygen generation in benzene". *J Chem Soc{,} Faraday Trans*. vol. 86, no. 14, pp. 2671–2, 1990.
[79] J.L. Charlton, R. Dabestani and J. Saltiel. "Role of triplet-triplet annihilation in anthracene dimerization". *Journal of the American Chemical Society*. vol. 105, no. 11, pp. 3473–6, 1983.
[80] S.M. Bachilo and R.B. Weisman. "Determination of Triplet Quantum Yields from Triplet−Triplet Annihilation Fluorescence". *The Journal of Physical Chemistry A*. vol. 104, no. 33, pp. 7711–4, 2000.
[81] S. Hoseinkhani, R. Tubino, F. Meinardi and A. Monguzzi. "Achieving the photon up-conversion thermodynamic yield upper limit by sensitized triplet–triplet annihilation". *Phys Chem Chem Phys*. vol. 17, no. 6, pp. 4020–4, 2015.
[82] B. Dick and B. Nickel. "Accessibility of the lowest quintet state of organic molecules through triplet-triplet annihilation; an indo ci study". *Chemical Physics*. vol. 78, no. 1, pp. 1–16, 1983.
[83] V. Gray, A. Dreos, P. Erhart, B. Albinsson, K. Moth-Poulsen and M. Abrahamsson. "Loss channels in triplet–triplet annihilation photon upconversion: importance of annihilator singlet and triplet surface shapes". *Physical Chemistry Chemical Physics*. vol. 19, no. 17, pp. 10931–9, 2017.
[84] M.A. Haidekker and E.A. Theodorakis. "Environment-sensitive behavior of fluorescent molecular rotors". *Journal of Biological Engineering*. vol. 4, no. 1, pp. 11, 2010.
[85] J.-H. Kang and E. Reichmanis. "Low-Threshold Photon Upconversion Capsules Obtained by Photoinduced Interfacial Polymerization". *Angewandte Chemie International Edition*. vol. 51, no. 47, pp. 11841–4, 2012.
[86] K. Moor, J.-H. Kim, S. Snow and J.-H. Kim. "[C70] Fullerene-sensitized triplet–triplet annihilation upconversion". *Chemical Communications*. vol. 49, no. 92, pp. 10829, 2013.
[87] S. Baluschev, V. Yakutkin, T. Miteva, G. Wegner, T. Roberts, G. Nelles, et al. "A general approach for non-coherently excited annihilation up-conversion: transforming the solar-spectrum". *New Journal of Physics*. vol. 10, no. 1, pp. 013007, 2008.
[88] T.W. Schmidt and F.N. Castellano. "Photochemical Upconversion: The Primacy of Kinetics". *The Journal of Physical Chemistry Letters*. vol. 5, no. 22, pp. 4062–72, 2014.
[89] D.J. Gisser, B.S. Johnson, M.D. Ediger and E.D. Von Meerwall. "Comparison of various measurements of microscopic friction in polymer solutions". *Macromolecules*. vol. 26, no. 3, pp. 512–9, 1993.
[90] N.B. Monardes. "Dos Libros/El vno que trata de todas las cosas que traen de nuestras Indias Occidentales que siruen al vso de Medicina y como se ha de vsar de la rayz de Mechoacan, purga excelentissima. El otro libro trata de dos medicinas marauillosas ...". Sevilla: en casa de Sebastian Trugillo; 1565.
[91] G.G. Stokes. "XXX. On the change of refrangibility of light". *Philosophical Transactions of the Royal Society of London*. vol. 142, pp. 463–562, 1852.
[92] R.W. Wood. "XXIX. Anti-Stokes radiation of fluorescent liquids". *The London,*

Edinburgh, and Dublin Philosophical Magazine and Journal of Science. vol. 6, no. 35, pp. 310–2, 1928.

[93] W. Chen, F. Song, S. Tang, G. Hong, Y. Wu and X. Peng. "Red-to-blue photon up-conversion with high efficiency based on a TADF fluorescein derivative". *Chem Commun*. vol. 55, no. 30, pp. 4375–8, 2019.

[94] S.H.C. Askes and S. Bonnet. "Solving the oxygen sensitivity of sensitized photon upconversion in life science applications". *Nature Reviews Chemistry*. vol. 2, no. 12, pp. 437–52, 2018.

[95] N.J. Turro, V. Ramamurthy and J.C. Scaiano. "Modern Molecular Photochemistry of Organic Molecules". Sausalito, California: University Science Books; 1110 p.2010.

[96] A. Monguzzi, R. Tubino and F. Meinardi. "Multicomponent Polymeric Film for Red to Green Low Power Sensitized Up-Conversion". *The Journal of Physical Chemistry A*. vol. 113, no. 7, pp. 1171–4, 2009.

[97] P.B. Merkel and J.P. Dinnocenzo. "Low-power green-to-blue and blue-to-UV upconversion in rigid polymer films". *Journal of Luminescence*. vol. 129, no. 3, pp. 303–6, 2009.

[98] S.H. Lee, J.R. Lott, Y.C. Simon and C. Weder. "Melt-processed polymer glasses for low-power upconversion via sensitized triplet–triplet annihilation". *J Mater Chem C*. vol. 1, no. 33, pp. 5142–8, 2013.

[99] A. Monguzzi, M. Mauri, M. Frigoli, J. Pedrini, R. Simonutti, C. Larpent, et al. "Unraveling Triplet Excitons Photophysics in Hyper-Cross-Linked Polymeric Nanoparticles: Toward the Next Generation of Solid-State Upconverting Materials". *The Journal of Physical Chemistry Letters*. vol. 7, no. 14, pp. 2779–85, 2016.

[100] T.J. Dougherty, C.J. Gomer, B.W. Henderson, G. Jori, D. Kessel, M. Korbelik, et al. "Photodynamic Therapy". *JNCI: Journal of the National Cancer Institute*. vol. 90, no. 12, pp. 889–905, 1998.

[101] F. Marsico, A. Turshatov, R. Peköz, Y. Avlasevich, M. Wagner, K. Weber, et al. "Hyperbranched Unsaturated Polyphosphates as a Protective Matrix for Long-Term Photon Upconversion in Air". *Journal of the American Chemical Society*. vol. 136, no. 31, pp. 11057–64, 2014.

[102] J.-H. Kim, F. Deng, F.N. Castellano and J.-H. Kim. "Red-to-Blue/Cyan/Green Upconverting Microcapsules for Aqueous- and Dry-Phase Color Tuning and Magnetic Sorting". *ACS Photonics*. vol. 1, no. 4, pp. 382–8, 2014.

[103] J. Jortner, S. Choi, J.L. Katz and S.A. Rice. "Triplet Energy Transfer and Triplet-Triplet Interaction in Aromatic Crystals". *Phys Rev Lett*. vol. 11, no. 7, pp. 323–6, 1963.

[104] N.A. Durandin, J. Isokuortti, A. Efimov, E. Vuorimaa-Laukkanen, N. V. Tkachenko and T. Laaksonen. "Efficient photon upconversion at remarkably low annihilator concentrations in a liquid polymer matrix: when less is more". *Chemical Communications*. 2018.

[105] E.M. Gholizadeh, L. Frazer, R.W. MacQueen, J.K. Gallaher and T.W. Schmidt. "Photochemical upconversion is suppressed by high concentrations of molecular sensitizers". *Phys Chem Chem Phys*. vol. 20, no. 29, pp. 19500–6, 2018.

[106] A. Monguzzi, J. Mezyk, F. Scotognella, R. Tubino and F. Meinardi. "Upconversion-induced fluorescence in multicomponent systems: Steady-state excitation power threshold". *Phys Rev B*. vol. 78, no. 19, pp. 195112, 2008.

[107] N. Durandin, J. Isokuortti, A. Efimov, E. Vuorimaa-Laukkanen, N. V. Tkachenko and T. Laaksonen. "Submitted". 2019.

[108] V. Gray, K. Moth-Poulsen, B. Albinsson and M. Abrahamsson. "Towards efficient solid-state triplet–triplet annihilation based photon upconversion: Supramolecular, macromolecular and self-assembled systems". *Coordination Chemistry Reviews*. vol. 362, pp. 54–71, 2018.

[109] T.N. Singh-Rachford and F.N. Castellano. "Pd(II) Phthalocyanine-Sensitized

Triplet−Triplet Annihilation from Rubrene". *The Journal of Physical Chemistry A*. vol. 112, no. 16, pp. 3550–6, 2008.

[110] J.L. Han, J. You, H. Yonemura, S. Yamada, S.R. Wang and X.G. Li. "Metallophthalocyanines as triplet sensitizers for highly efficient photon upconversion based on sensitized triplet–triplet annihilation". *Photochem Photobiol Sci*. vol. 15, no. 8, pp. 1039–45, 2016.

[111] J. Han, F. Zhang, J. You, Y. Hiroaki, S. Yamada, T. Morifuji, et al. "The first transition metal phthalocyanines: sensitizing rubrene emission based on triplet–triplet annihilation". *Photochem Photobiol Sci*. vol. 16, no. 9, pp. 1384–90, 2017.

[112] Y. Che, W. Yang, G. Tang, F. Dumoulin, J. Zhao, L. Liu, et al. "Photophysical properties of palladium/platinum tetrasulfonyl phthalocyanines and their application in triplet–triplet annihilation upconversion". *J Mater Chem C*. vol. 6, no. 21, pp. 5785–93, 2018.

[113] F. Ghani, J. Kristen and H. Riegler. "Solubility Properties of Unsubstituted Metal Phthalocyanines in Different Types of Solvents". *Journal of Chemical & Engineering Data*. vol. 57, no. 2, pp. 439–49, 2012.

[114] R.R. Islangulov, D. V Kozlov and F.N. Castellano. "Low power upconversion using MLCT sensitizers". *Chem Commun*. no. 30, pp. 3776–8, 2005.

[115] Q. Zhou, M. Zhou, Y. Wei, X. Zhou, S. Liu, S. Zhang, et al. "Solvent effects on the triplet–triplet annihilation upconversion of diiodo-Bodipy and perylene". *Physical Chemistry Chemical Physics*. vol. 19, no. 2, pp. 1516–25, 2017.

[116] W. Wu, X. Cui and J. Zhao. "Hetero Bodipy-dimers as heavy atom-free triplet photosensitizers showing a long-lived triplet excited state for triplet–triplet annihilation upconversion". *Chem Commun*. vol. 49, no. 79, pp. 9009–11, 2013.

[117] W. Wu, H. Guo, W. Wu, S. Ji and J. Zhao. "Organic Triplet Sensitizer Library Derived from a Single Chromophore (BODIPY) with Long-Lived Triplet Excited State for Triplet–Triplet Annihilation Based Upconversion". *The Journal of Organic Chemistry*. vol. 76, no. 17, pp. 7056–64, 2011.

[118] C. Zhang, J. Zhao, S. Wu, Z. Wang, W. Wu, J. Ma, et al. "Intramolecular RET Enhanced Visible Light-Absorbing Bodipy Organic Triplet Photosensitizers and Application in Photooxidation and Triplet–Triplet Annihilation Upconversion". *Journal of the American Chemical Society*. vol. 135, no. 28, pp. 10566–78, 2013.

[119] T.N. Singh-Rachford, A. Haefele, R. Ziessel and F.N. Castellano. "Boron Dipyrromethene Chromophores: Next Generation Triplet Acceptors/Annihilators for Low Power Upconversion Schemes". *Journal of the American Chemical Society*. vol. 130, no. 48, pp. 16164–5, 2008.

[120] X. Cui, J. Zhao, P. Yang and J. Sun. "Zinc(ii) tetraphenyltetrabenzoporphyrin complex as triplet photosensitizer for triplet–triplet annihilation upconversion". *Chem Commun*. vol. 49, no. 87, pp. 10221–3, 2013.

[121] T. V Esipova, H.J. Rivera-Jacquez, B. Weber, A.E. Masunov and S.A. Vinogradov. "Stabilizing g-States in Centrosymmetric Tetrapyrroles: Two-Photon-Absorbing Porphyrins with Bright Phosphorescence". *The Journal of Physical Chemistry A*. vol. 121, no. 33, pp. 6243–55, 2017.

[122] A.E. Siegman. "How to (Maybe) Measure Laser Beam Quality". In: DPSS (Diode Pumped Solid State) Lasers: Applications and Issues. Optical Society of America; p. 184–991998.

[123] A. Ogunsipe, D. Maree and T. Nyokong. "Solvent effects on the photochemical and fluorescence properties of zinc phthalocyanine derivatives". *Journal of Molecular Structure*. vol. 650, no. 1, pp. 131–40, 2003.

[124] J. Olmsted. "Calorimetric determinations of absolute fluorescence quantum yields". *The Journal of Physical Chemistry*. vol. 83, no. 20, pp. 2581–4, 1979.

[125] G.A. Crosby and J.N. Demas. "Measurement of photoluminescence quantum yields. Review". *The Journal of Physical Chemistry*. vol. 75, no. 8, pp. 991–1024, 1971.

[126] A.Y. Lebedev, A. V Cheprakov, S. Sakadžić, D.A. Boas, D.F. Wilson and S.A.

Vinogradov. "Dendritic Phosphorescent Probes for Oxygen Imaging in Biological Systems". *ACS Applied Materials & Interfaces*. vol. 1, no. 6, pp. 1292–304, 2009.

[127] A. Harriman. "Luminescence of porphyrins and metalloporphyrins. Part 1.—Zinc(II), nickel(II) and manganese(II) porphyrins". *J Chem Soc{,} Faraday Trans 1*. vol. 76, no. 0, pp. 1978–85, 1980.

[128] C.A. Parker and C.G. Hatchard. "Triplet-singlet emission in fluid solutions. Phosphorescence of eosin". *Trans Faraday Soc*. vol. 57, no. 0, pp. 1894–904, 1961.

[129] F.B. Dias, T.J. Penfold and A.P. Monkman. "Photophysics of thermally activated delayed fluorescence molecules". *Methods and Applications in Fluorescence*. vol. 5, no. 1, pp. 12001, 2017.

[130] Y. Im, M. Kim, Y.J. Cho, J.-A. Seo, K.S. Yook and J.Y. Lee. "Molecular Design Strategy of Organic Thermally Activated Delayed Fluorescence Emitters". *Chemistry of Materials*. vol. 29, no. 5, pp. 1946–63, 2017.

[131] M. Baroncini, G. Bergamini and P. Ceroni. "Rigidification or interaction-induced phosphorescence of organic molecules". *Chem Commun*. vol. 53, no. 13, pp. 2081–93, 2017.